Chapter 8.

Chemical reactions in hydrothermal systems.

October_9_2016.

8.1. Introduction.

In Chapter 1 we proposed that hydrothermal mineralising systems are giant chemical reactors held far from equilibrium by the influx of fluids and heat. As such they are open thermodynamic systems that evolve with time towards one or more *non-equilibrium stationary states*. A stationary state is one where there is no change of a particular measure of the system, such as composition or temperature, with time. Stationary states are commonly referred to as *steady states*; we prefer the term stationary state since such states can be unstable under a small perturbation and oscillate in both time and space or evolve to a new stationary state. In this regard hydrothermal systems differ from many metamorphic systems that remain closed and hence must evolve towards an *equilibrium stationary state* although the evolution towards an equilibrium state may be quite complicated. The purpose of this chapter is to elaborate upon these concepts and indicate the basic principles on which the behaviour of such open flow chemical reactors are based. In doing so we adopt an approach that might be taken by a chemical engineer whose goal is to design and operate a chemical reactor that produces the maximum possible yield given constraints placed upon him by infrastructure requirements and the physical-chemical processes that operate.

The chapter is essentially an atlas of diagrams that illustrates the principles that govern mineral reactions in open hydrothermal systems. We do not concentrate on the mathematics behind these diagrams. The interested reader is referred to the reading list at the end of the chapter. Since the rates of mineral reactions in open systems are controlled by the rates of supply of reactants and of heat we first need to examine the characteristics of three fundamental processes that are involved in the formation of hydrothermal mineralising systems. These are: (i) the differences between metamorphic and hydrothermal systems; these include in particular the temperature changes arising from the exothermic nature of the alteration mineral reactions; (ii) the heterogeneity in the fluid flow system and (iii) the equal volume (pseudomorphic) nature of most of the mineral reactions; this latter process not only controls the character of the mineral reactions but also controls the competition between consumption and supply of reactants and heat.

The temperature changes associated with exothermic mineral reactions are also important from a mechanical point of view since they result in changes in fluid pore pressure and hence influence the effective stress. We will see (particularly in Chapter 12) that temperature changes are typically oscillatory in hydrothermal systems so that changes in effective stress are also oscillatory which leads to the familiar crack-seal microstructures in veins. If the hydrothermal reactions involve devolatilisation then oscillations in effective stress are enhanced and oscillatory formation of breccias and/or fluidisation occurs. The combination of oscillations in temperature and fluid pressure also leads to gold and quartz deposition during the relaxation phase of each oscillation; we look at this in greater detail in Chapter 12. Thus the nonlinear behaviour of mineral reactions and their strong dependence on flow rates and thermal energy supply leads to a rich system of mechanical/chemical behaviour which is responsible for the heterogeneity and characteristic structures and mineral assemblages we observe in hydrothermal systems. The two routes to these structures and mineral assemblages (one via exothermic reactions and the other via endothermic

devolatilisation reactions) are shown in Figure 8.1 and we elaborate on various aspects of this diagram in the remainder of this chapter.

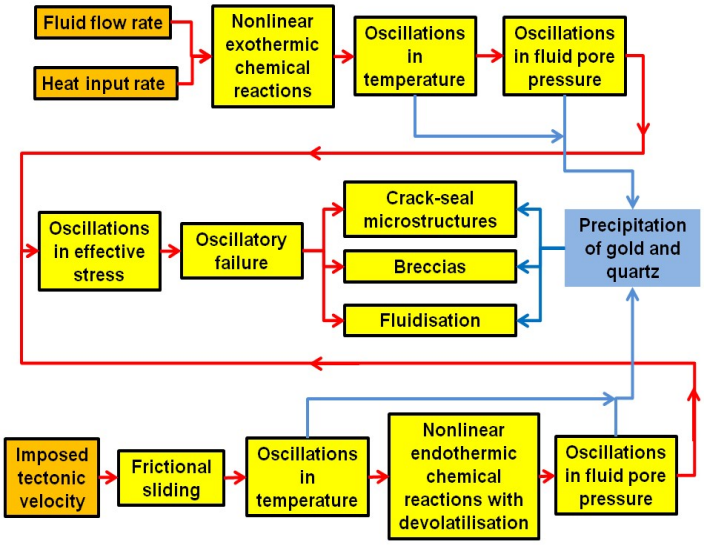

Figure 8.1. Flow chart showing many of the feedback processes that operate in hydrothermal systems to produce veining and brecciation together with precipitation of gold and quartz. The externally imposed forcing processes are shown in orange boxes. The chemical and mechanical processes are shown in yellow boxes and the processes leading to gold and quartz precipitation are shown as blue arrows and box. There are two routes to the observed microstructures and precipitation processes. One is via exothermic mineral reactions that are driven by heat and fluid supply. The other is via endothermic devolatilisation mineral reactions that are driven by heat supplied from mechanical deformation. Both produce oscillations in temperature and fluid pressure. The oscillations in fluid pressure lead to oscillations in effective stress and hence to oscillatory modes of failure. The thermal/fluid pressure relaxation phase associated with each oscillation leads to quartz and gold deposition.

8.1.1. The differences between hydrothermal and metamorphic systems.

It is fundamental in understanding hydrothermal systems to make clear distinctions between the processes and time scales that operate in such systems as opposed to such processes and time scales in regional metamorphic systems. A hydrothermal system differs from a regional metamorphic system in the following fundamental aspects:

(i) Hydrothermal systems are open flow, rather than closed, thermodynamic systems (Ord et al., 2012). This means that the mineral reaction rates depend on the supply of chemical components and of heat to the system. In metamorphic systems that are closed this is still true but the supply problem is internal to the system and hence on a local grain-size scale, perhaps measured in a few millimetres at most (Carmichael, 1969). In hydrothermal systems fluid flow into, through and out of the system is driven by regional and local pore pressure gradients induced by an imposed fluid flux, which may be episodic, on the boundaries of the system but modified locally by fluid pressure fluctuations induced by temperature changes and by both plastic and chemical dilatancy. These effects are important in hydrothermal systems since coupling of pore pressure to temperature fluctuations is a fundamental process and strongly influences local variations in pore pressure distribution and hence the local equilibrium solubility of gold (Loucks and Mavrogenes, 1999).

(ii) The time scale involved in producing mineralised systems is at least an order of magnitude smaller than in metamorphic systems; 1 to 2 million years seems an upper limit for the formation of a mineralised hydrothermal system (Silberman et al., 1972; Goldfarb et al., 1991; McInnes et al. 2005 a, b; Simmons and Brown, 2006; Fu et al., 2010; Yardley and Cleverley, 2016) whereas 10 to 40 million years seems a lower limit for metamorphic systems (Connolly and Thompson, 1989). The importance of this issue becomes apparent when we consider heat production/absorption rates within hydrothermal systems arising from exothermic/endothermic mineral reactions. In metamorphic systems the rates of release or absorption of heat from mineral reactions integrated over time scales greater than a few million years is comparable to or less than the background radiogenic crustal heat production (Connolly and Thompson, 1989). In hydrothermal systems the heat production rates integrated over time scales less than or equal to a million years exceed the background radiogenic heat production rates and have an important influence on temperature and hence on reaction rates and on fluid pressure (see Chapter 2, Figure 2.17).

(iii) Metamorphic rocks, especially those formed in prograde metamorphic conditions, typically show little sign of brittle behaviour and presumably behave as elastic-plastic-viscous materials with little if any plastic-viscous dilatancy arising from mechanical deformation. Thus mechanical volume changes arise only from elasticity and hence local fluid fluxes are driven by gradients in mean stress (Detournay and Cheng, 1993; Hobbs and Ord, 2016). Chemically induced volume changes in both metamorphic and metasomatic rocks are accommodated by plastic-viscous flow and the pore pressure gradients induced by such chemical compaction/expansion processes may outweigh the elastic mean stress gradients. By contrast, hydrothermal systems are dominated by brittle deformations so that plastic dilatancy, together with chemical dilatancy, is a characteristic constitutive response of the system. These deformations are also exothermic and hence there is an accompanying temperature effect on pore pressure (Ghabezloo and Sulem, 2009).

(iv) Metamorphic systems are proposed to be closed thermodynamic systems so that dissipation of energy during the evolution of the system results from processes internal to the system. As such the second law of thermodynamics says the evolution is towards an equilibrium stationary state where, if the reactions have proceeded to completion, the mineral assemblages are defined by the phase rule. Such a statement needs to be modified if the metamorphic system is open such as in hydrating retrogressive metamorphism and in devolatilising and melting systems where fluids enter and/or escape from the system. These systems resemble hydrothermal systems but the long time periods involved imply that even these systems become closed and hence must approach an equilibrium state. Hydrothermal systems by contrast remain open throughout their lifetime and the evidence indicates that the mean temperature increases as the system evolves. Examples are given in Barnicoat et al. (1997), Henley and Berger (2000 and references therein). The chemical and mineralogical evolution of these systems is controlled by the rates at which mineral reactions proceed which in turn depend on the rates of temperature change and of fluid supply (Bilous and Amundson, 1955;

Aris, 1961, 1978, 1989; Gray and Scott, 1990). Such evolving open systems are characterised by a paragenetic sequence reflecting the initiation and extinction of the growth of different mineral phases as both the temperature and flow rates change. Hydrothermal mineral assemblages sometimes obey the open system phase rule proposed by Korzhinskii (1959) but commonly heterogeneity and overprinting microstructures mean that such approaches are not applicable.

In such evolving non-equilibrium systems the mineral assemblage is characterised by the presence of stable, non-equilibrium mineral phases rather than stable equilibrium phases. The rules for determining such stable non-equilibrium phases have long been known to chemical engineers (Warden et al., 1964 a, b; Parmon, 2010) but we will not discuss these rules here. The point is that the paragenetic sequence represents a series of overprinting stable, non-equilibrium assemblages that record the evolution of the hydrothermal system.

8.1.2. Heterogeneity.

All hydrothermal systems are heterogeneous in their structure; this heterogeneity is expressed as the presence of breccias or veins or diffuse regions of higher than average permeability. In Figure 8.2 we consider a region comprised of quartz diorite 10 km x 10 km with boundaries fixed at 300°C. A pore pressure gradient is imposed equivalent to a lithostatic gradient from left to right. The background permeability of the model is 10^{-17} m^2 and lenses of various shapes and sizes with a permeability of 10^{-15} m^2 are embedded in the model. A Darcy fluid flux of 2.65 x 10^{-10} m s^{-1} is imposed at the left hand margin. The heat production rate within the lenses is 7.684 x 10^9 J m^{-3} of rock (as in Figure 2.17) and the alteration reaction is allowed to run for 10^4 years before being turned off so that the heat production rate during that time is 2.43 x 10^{-3} W m^{-3}; each lens therefore behaves as a chemical reactor. The model shows that (i) some regions are fed almost solely by the imposed boundary flux whereas others are fed by fluids expelled from neighbouring reactors (Figure 8.2 a); (ii) The distribution and magnitude of the fluid flux in each reactor depends on its size and shape and on its position within the overall geometry (Figure 8.2 b); (iii) the temperature within each reactor is a function of its size and shape (Figure 8.2 c); (iv) the combination of fluid flux and temperature again varies with the size and shape of the reactor and its position in the overall geometry (Figure 8.2 d). It is important in considering chemical reactions in hydrothermal systems that heterogeneity in the distribution of fluid flow velocity is the norm rather than an exception.

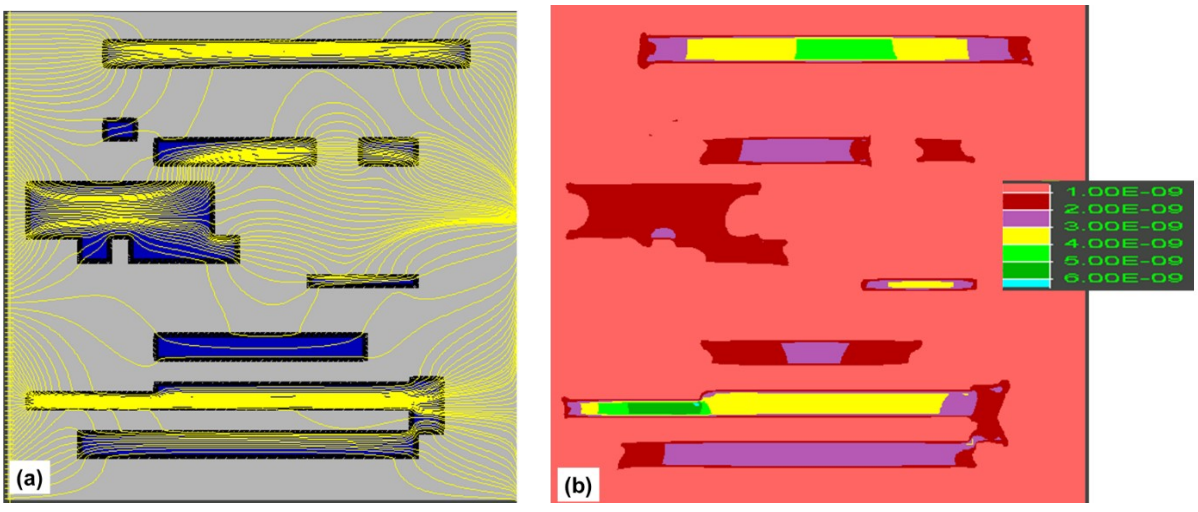

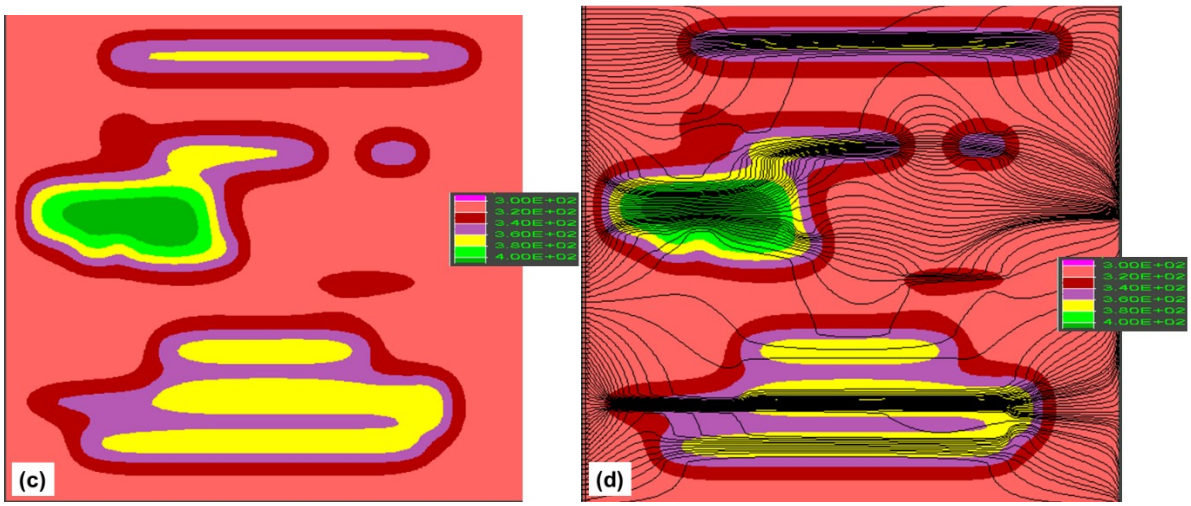

Figure 8.2. Heterogeneity in fluid flow and temperature in a regional scale hydrothermal system. A region 10 km x 10 km and ambient temperature of 300°C is exposed to a fluid flux on the left hand side. The background permeability is 10^{-17} m^2 and higher permeability patches (10^{-15} m^2) are included as indicated by the dark blue areas in (a). The rock is considered to be quartz diorite with alteration to a quartz-muscovite assemblage in the high permeability areas according to Table 2.2. The situation is shown at the end of 10^4 years. (a) Streamlines (yellow) superimposed on the permeability distribution. (b) Magnitudes of the Darcy flow velocity. Legend gives velocity im m s^{-1} (c) Temperature distribution. Legend gives temperature in °C. (d) Temperature distribution with superimposed streamlines (black). The model incorporates complete coupling between fluid flow and thermal transport.

8.1.3. Constant volume mineral reactions and their implications.

In Figure 1.8 we show an example of sericite plus quartz alteration replacing a finely layered chlorite rich rock. There is no displacement or distortion of the layering arising from the replacement reactions. This indicates that the replacement process is a constant volume process. Such constant volume mineral reactions are a ubiquitous feature of mineralising systems and are common as pseudomorphic reactions in both metamorphic and hydrothermal environments; they have been described and documented in hydrothermal systems since Lindgren in 1912. Constant volume reactions carry a number of implications for hydrothermal systems that are not commonly considered in metamorphic systems.

A simple example is the replacement of sphalerite by covellite. If this is written with regard only for a balance of molecular units as is the common convention we write:

$$ZnS + Cu^{2+} + SO_4^{2-} \rightarrow CuS + Zn^{2+} + SO_4^{2-} \qquad (8.1)$$

The volume of one unit formula of ZnS is 39.37 $\mathring{A}^3$ whilst that of covellite is 34.24 $\mathring{A}^3$. Thus the above reaction represents a 15% loss in volume. If one were to preserve the balance of molecular units but preserve volume, the reaction is written:

$$20ZnS + 23Cu^{2+} + 23SO_4^{2-} + 3H_2S \rightarrow 23CuS + 20Zn^{2+} + 23SO_4^{2-} + 6H^+ \qquad (8.2)$$

An important difference between (8.1) and (8.2), other than the differences in volume change, is that reaction (8.2) produces H^+ whereas (8.1) does not.

Consider the reaction:

$$13Cu_2S + 24Cu^{2+} + 69SO_4^{2-} + 30Fe^{3+} + 52H_2O \rightarrow 50Cu + 30Fe^{2+} + 82SO_4^{2-} + 104H^+ \qquad (8.3)$$

This involves a volume change of 0.85% ; again H^+ is produced and the system is also autocatalytic in SO_4^{2-} with 69 molecules of SO_4^{2-} on the left hand side producing 82 molecules on the right hand side. These two features, namely the production of H+ and the autocatalytic production of SO_4^{2-} are characteristic of many constant volume reactions involving sulphides and do not appear if the same reactions are written preserving mass alone.

In some reactions that preserve volume the system is autocatalytic or auto-inhibitory in the conversion of Fe^{3+} to Fe^{2+}. An example, involving a 0.16 % volume change, is

$$31Cu_2S + 62Fe^{3+} + 9S^{2-} \rightarrow 20CuFeS_2 + 42Cu^{2+} + 42Fe^{2+}$$

Many other examples of constant volume reactions are given in the recommended reading at the end of the chapter.

Another important characteristic of constant volume replacement reactions is the implication for periodic or chaotic growth rates. Consider the replacement of calcite by dolomite due to the influx of Mg^{2+} from an outside source (Figure 8.3). If the replacement is constant volume in character then the rate of dissolution of calcite is equal to the rate of growth of dolomite. The dissolution of calcite occurs according to

$$CaCO_{3\,(solid)} \rightarrow Ca^{2+} + CO_3^{2-}$$

whereas the growth of dolomite occurs according to

$$Ca^{2+} + Mg^{2+} + 2\,CO_3^{2-} \rightarrow CaMg(CO_3)_{2\,(solid)}$$

The mass balance arising from these two reactions in order to generate a constant volume replacement is

$$1.74\ CaCO_{3(solid)} + Mg^{2+} + 0.26\,CO_3^{2-} \rightarrow CaMg(CO_3)_{2(solid)} + 0.74Ca^{2+}$$

One can show (see recommended reading) that the growth rate of dolomite, $R_{dolomite}$, is given by a relation that involves exponential dependence on time, t, and on the activity of Mg^{2+}, a_{Mg2+}, added to the system:

$$R_{dolomite} = A\,(a_{Mg2+})\,\exp(t/\tau)$$

where A is a constant (involving a_{Ca2+}) and τ is a time constant that depends on a_{Mg2+}.

Thus the growth rate of dolomite is exponential with time and depends on the supply of Mg^{2+}. If we assume Mg^{2+} is added at a constant rate then the exponential growth rate of dolomite ultimately outstrips the supply of Mg^{2+} and dolomite growth stops until the activity of Mg^{2+} in the system can build up again when the whole process repeats. If the supply of Mg^{2+} is not constant and varies because it depends on other reactions in the system then the growth rate of dolomite become chaotic. The conclusion is that the ubiquitous presence of constant volume replacement reactions in hydrothermal systems implies at least periodic growth rates and probably chaotic growth rates. These varying growth rates are reflected in compositional zoning in many sulphides such as pyrite and sphalerite.

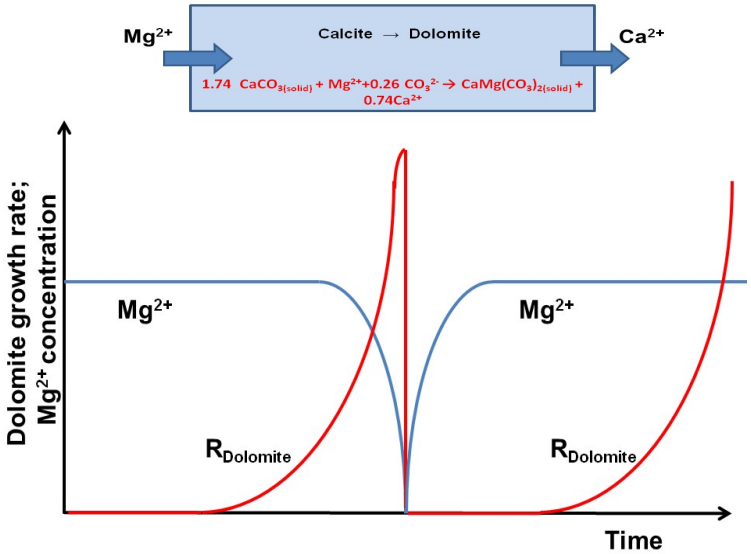

Figure 8.3. Equal volume replacement of calcite by dolomite. Modified from Merino and Canals (2011). The constant volume constraint means that the growth rate of dolomite is exponential and ultimately outstrips the supply of Mg^{2+}. The growth of dolomite then stops until the activity of Mg^{2+} in solution can build up again. The process then repeats in a periodic fashion.

8.2. The basic principles governing mineral reactions in open flow systems.

The general energy balance for an open flow chemical reactor is shown in Figure 8.4. Mass, energy and chemical concentrations of the reacting species are added at one or more places in the reactor and chemical reactions take place within the reactor, of volume V, to produce outflows of mass energy and chemical concentrations. Simultaneously heat is added or removed from the country rocks and the displacements in the surrounding rocks do work in deforming the system by brecciation, dilation and fracturing. Energy is generated or consumed in the reactor by both chemical reactions, deformation and fluid flow. The energy balance for the reactor is given by

$$\begin{bmatrix}\text{Rate of energy}\\ \text{accumulation}\end{bmatrix} = \begin{bmatrix}\text{Rate of energy}\\ \text{entering system}\\ \text{by inflow}\end{bmatrix} - \begin{bmatrix}\text{Rate of energy}\\ \text{leaving system}\\ \text{by outflow}\end{bmatrix} + \begin{bmatrix}\text{Rate of heat}\\ \text{added to system}\end{bmatrix} + \begin{bmatrix}\text{Rate of work}\\ \text{done on and in the system by}\\ \text{deformation}\end{bmatrix} \tag{8.4}$$

The overall yield of the reactor is governed by the ways in which these various processes interact. The aim of this section is to spell out these interactions in the simplest possible form. We consider the deformation term in Section 8.5.

Below we define three terms that are convenient in describing the behaviour of chemical reactors. The first convenient quantity is the residence time, τ, which is the average time a fluid particle spends in the reactor.

$$\tau = V / q = V\phi / \hat{V}$$

where q is the volumetric flow rate into the reactor, $\hat{V}$ is the Darcy velocity and ϕ is the porosity. As an example if the system is a cube, 1km on edge, and the Darcy velocity is 10^{-8} m s^{-1} with an average porosity of 10^{-1} the residence time is 10^{10} s or $\approx$ 317 years. In a massive alteration system 10 km on edge the equivalent residence time is $\approx$ 3170 years.

The second term is the reaction extent, ξ, which is a measure of how far a particular mineral reaction has proceeded since initiation. If the reaction is A $\rightarrow$ B and the concentrations of A and B are written a and b then $a_0 + b_0 = a + b$ where a_0, b_0 are the initial concentrations of A and B then the extent, ξ, of the reaction is

$$\xi = \frac{a_0 - a}{a_0}$$

so that $\xi = 0$ when the reaction begins and $a = a_0$ and $\xi = 1$ when the reaction is completed and $a = 0$.

We also note that the rate, k_i, of the i^{th} mineral reaction is exponentially dependent on temperature, T, according to

$$k_i = k_{i0} \exp(-E_i / R\,T)$$

where k_{i0} is a reference reaction rate for the i^{th} reaction, E_i is the activation energy for the i^{th} reaction and R is the gas constant.

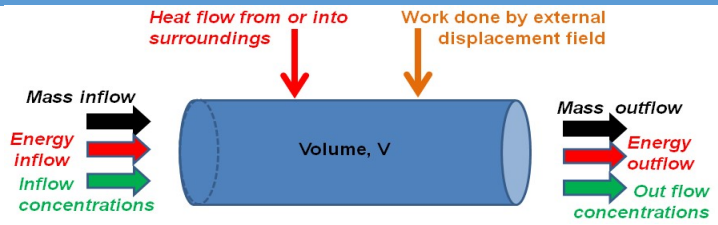

Figure 8.4. The energy balance in a chemical reactor (mineral system). The objective of the mineral reactor engineer is to adjust these parameters so that the maximum yield (ore grade) is achieved.

8.2.1. The influence of temperature and heat production on reactor behaviour.

The basic chemical arguments that control the characteristics of a mineral system are straight-forward. We begin (as did the chemical engineers with an argument put forward by van Heerden in 1953) by considering the influence of temperature and heat production on reactor behaviour. Consider a reaction that proceeds by itself once, using the heat liberated by the reaction, some critical temperature is reached (the ignition temperature); such reactions are said to be *autothermic*. The behaviour of all autothermic exothermal reactions follows the same principles and is exemplified by the ignition of a camp fire. Although the system may be slow to start (the analogy is a camp fire that smoulders before ignition) ultimately a steady state is reached where the heat consumption is balanced by the heat production. The fractional conversion of reactants varies rapidly with temperature in a nonlinear manner. The reaction starts slowly, then accelerates and reaches maximum conversion at which stage the reaction rate and heat production reach a steady state corresponding to maximum yield for the reaction. The plot of heat production rate versus temperature is shown in Figure 8.5 (a) by the red curve for a given feed rate or residence time. However the heat consumed which is a combination of heat produced and heat lost to the wall rocks is approximately a linear function of temperature and is shown in Figure 8.5 (a) by the blue lines. If the heat consumption is large (curve A) then no reaction occurs; the fire never ignites). For the heat consumption represented by the line B there are two intersections with the heat production curve at S (which is a steady state condition) and at I_1 (which represents ignition for these conditions). The ignition condition is unstable (a smouldering or intermittent fire) and ultimately evolves to S (a roaring, successful fire). For slow rates of heat consumption (represented by the line C) there is one intersection at I_2 which represents ignition for these conditions but the system never reaches a steady state (the fire smoulders).

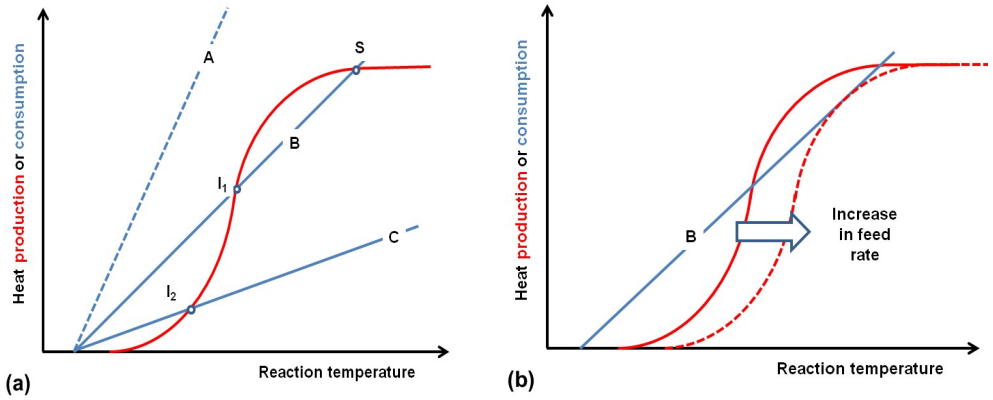

Figure 8.5. The behaviour of autothermic, irreversible exothermal mineral reactions.

The influence of feed rate on this behaviour is shown in Figure 8.5 (b) for the curve B in (a). Feed rate does not significantly change the heat consumption line but the heat production curve is shifted to the right (higher temperatures). Ultimately the heat consumption line just touches the heat production line as in Figure 8.5 (b) and for feed rates

larger than this there is no reaction; for these conditions the fire is blown (or snuffed) out. Thus there exists a delicate balance between heat production, heat consumption and feed rate that optimises the yield of such reactors. The lesson to be learnt is that high flow rates do not necessarily make a large high grade ore body; the flow rates have to be matched with heat production and consumption in order to optimise the yield.

The arguments presented above involving Figure 8.5 apply to irreversible reactions. If the reaction is reversible then the heat production curve is different and represented in Figure 8.6 (a). The same kind of arguments apply as in Figure 8.5 except that steady state conditions can now be achieved for slow heat consumption conditions (line C in Figure 8.6 (a) corresponding to steady state S_2).

Figure 8.6 (b) shows a similar curve but now the axes are reaction rate and flow rate on the ordinate and residence time on the abcsissa. This particular curve is drawn for a situation where some of the reactant added in the inflow stream is initially present in the reactor. There are now three stationary states: A (low yield and stable); B (moderate yield and unstable) and C (higher yield and stable). This diagram is shown in a different form in Figure 8.7.

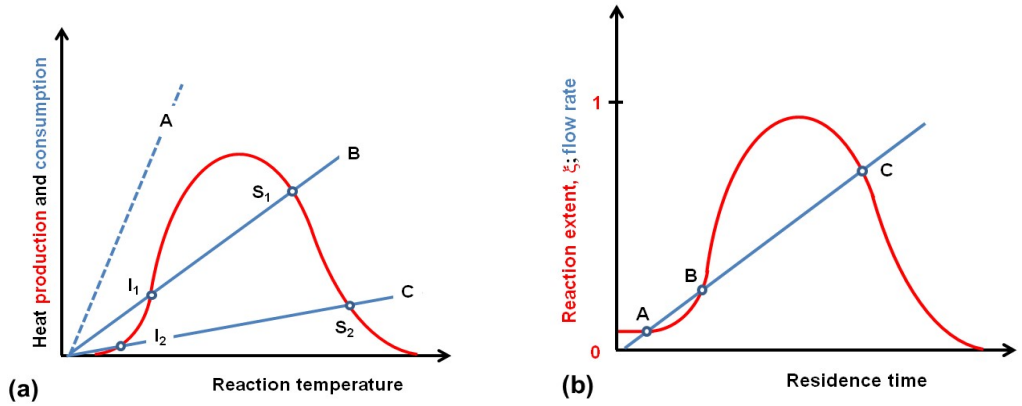

Figure 8.6. The behaviour of autothermic, reversible exothermal mineral reactions. (a) Heat budget plotted against reaction temperature. Line A represents high rates of heat consumption and the reaction never ignites. Line B represents internediate rates of heat consumption and high rates of steady state heat generation are achieved at S_1. For low rates of heat consumption (line C) low rates of steady state heat production, S_2, are achieved at high reaction temperatures. In both situations where reactions ignite (I_1 and I_2) the states are unstable. (b) Flow rate and reaction rate plotted against residence time.

There are a number of other ways of expressing the influence of temperaure and heat production on the behaviour of reactions. We have seen that the presence of an unstable and a stable stationary state for a given flow rate is characteristic of many reactions. We see this again in plots of the extent of a reaction, ξ, against the residence time in Figure 8.7 and the plot of reactor temperature against residence time in Figure 8.8. These curves are representative of a large number of processes that occur in nonlinear systems and hydrothermal systems in particular. Both Figures 8.7 and 8.8 show the development of what are called S-curves where the reaction extent (in Figure 8.7) and the reactor temperure (in Figure 8.8) show two values for a given residence time. These S-curves develop for exothermic reactions with relatively large activation energies. For low (or zero) activation energies (reactions with activation energies smaller than -10 kJ/kmol) and for endothermic reactions the curves are single valued for a given residence time and become sygmoidal in shape for low activation energies and for endothermic reactions.

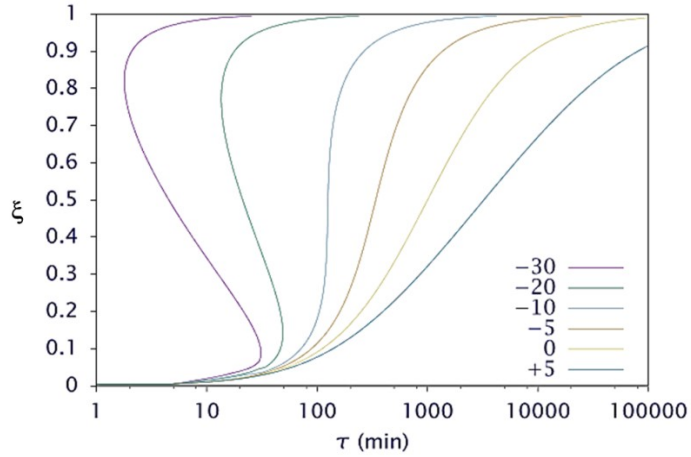

Figure 8.7. Plot of extent of reaction against residence time for different values of the activation energy ($\Delta H \times 10^{-4}$ kJ/kmol) for the reaction.

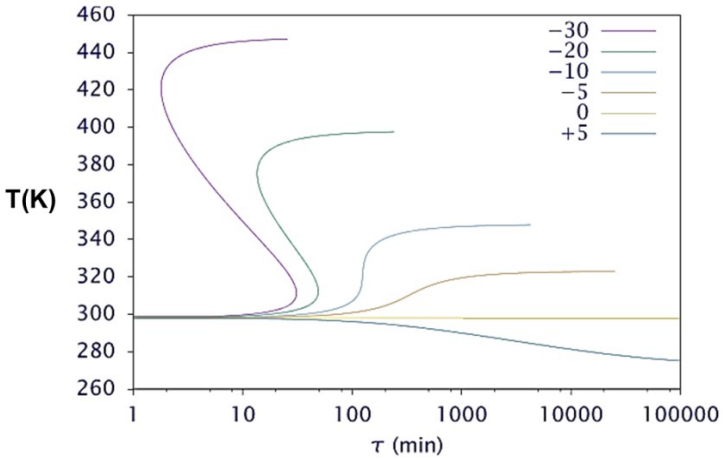

Figure 8.8. Plot of reactor temperature against residence time for different values of the activation energy ($\Delta H \times 10^{-4}$ kJ/kmol) for the reaction.

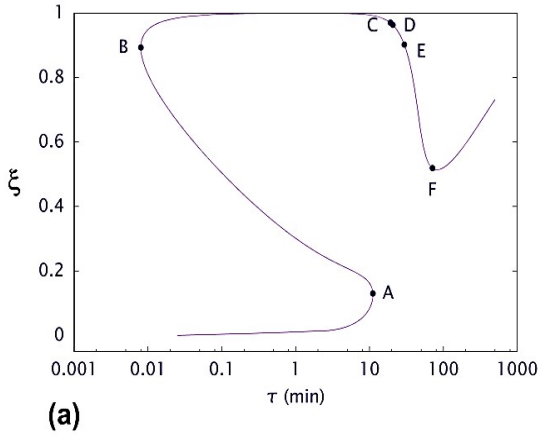

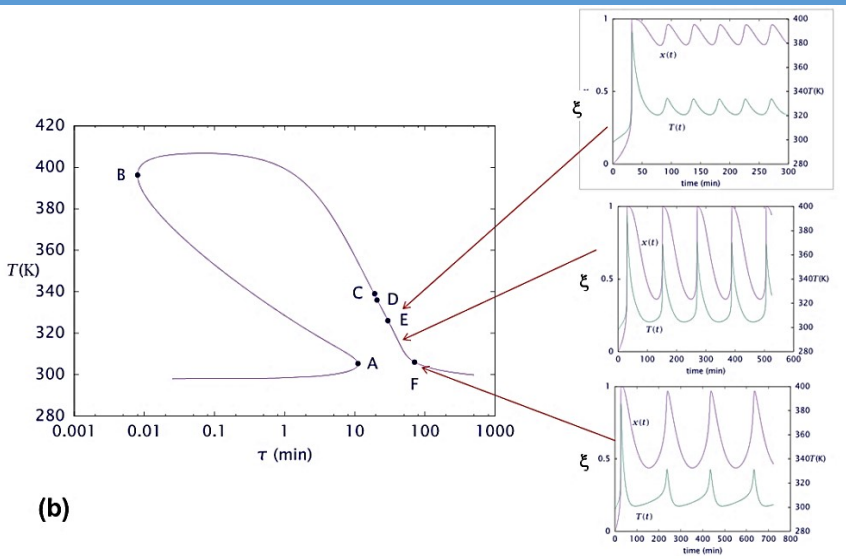

Figure 8.9. Illustrations of reaction behaviour for the exothermic reaction A → B. (a) Extent of reaction vs residence time. (b) Temperature vs residence time on left and plots of reaction extent and temperature vs time (on right) for various values of the residence time.

If the activation energy for the reaction is increased the S-curves of Figures 8.7 and 8.8 evolve into "mushroom" shaped curves of Figure 8.9. Many states on these figures are unstable and examples are shown for the variations of reaction extent and temperature with time in the right hand panel of Figure 8.9 (b).

A different type of diagram is shown in Figure 8.10. Here the extent of the reaction is plotted against the dimensionless temperature, T/*J*, of the reactor (the actual temperature, T, divided by $J = -\dfrac{\Delta H}{c_P}$ where ΔH is the activation energy of the reaction and c_P is the specific heat at constant pressure). We define a quantity, μ, which is a measure of the heat loss from the reactor. The diagram on the left of Figure 8.10 is for $\mu = 0$ whereas the bank of diagrams on the right of Figure 8.10 shows similar plots but with values of μ between 0.5 and 7.5. The three points A, B and C correspond to the same points in Figure 8.6 (b). Point A corresponds to a stable stationary state with low reaction yield at a low reactor temperature. Point B corresponds to an unstable stationary state with moderate reaction yield and medium temperature. Point C corresponds to a stable stationary state with high reaction yield and high reactor temperatures.

The dashed curve EBD is known as a *separatrix* and separates reaction trajectories that eventually evolve to A from those that eventually evolve to C. The diagram illustrates a fundamental aspect of chemical reactors: those reactions that are designed to reach full reaction yield at ξ = 1 and begin at temperatures corresponding to the point I evolve to a low yield and a low temperature state at A whereas those that begin at J (just slightly higher in temperature than I) evolve to a high yield and high temperature state at C. Thus the behaviour of the reactor and the yield of the reactor is highly sensitive to the initial conditions imposed on the reactor and it is possible for the reactor yield to vary dramatically in space simply because of initial, small heterogeneities in temperature.

The change in the behaviour of the reactor as μ is increased is shown in the right hand panel of Figure 8.10. A and C approach B as μ is increased and finally collapse onto B which evolves to a stable attractor for the system. This means that although high yields are possible

for low values of μ and suitable initial temperatures, moderate yields are the only possibility for large values of μ.

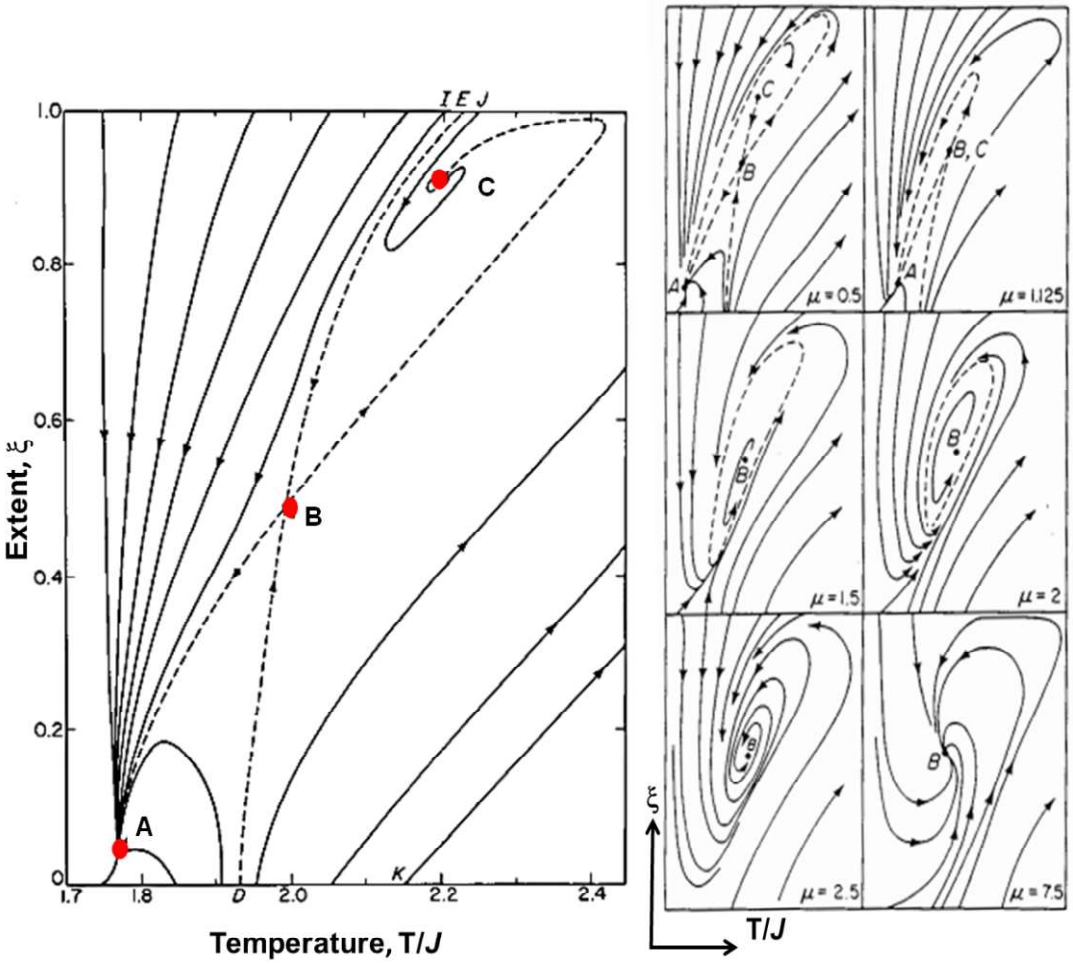

Figure 8.10. Plots of extent of reaction, ξ, vs dimensionless temperature, T/*J*, for a reaction with three stationary states. Left hand diagram, no heat loss from the system. A is a low yield and low temperature stable stationary state. B is an intermediate yield, intermediate temperature unstable stationary state and C is a high yield high temperature stable stationary state. All systems with initial conditions to the left of the line EBD evolve to the stationary state C. All systems with initial conditions to the right of the line EBD evolve to the stationary state A. In the right panel the system is shown with various degrees of heat loss indicated by the parameter, μ. As μ is increased the stationary states A and C collapse onto B which ultimately becomes a stable attractor. For intermediate values of μ the system oscillates around B.

8.2.2. Influence of flow rates (residence time) on reaction yield.

The arguments presented for Figures 8.5 and 8.6 apply to more complicated systems except that more than one steady state may occur and multiple unstable states may exist. We can also frame the arguments in terms of flow rates rather than in terms of heat production and consumption rates. In an open flow isothermal system (Figure 8.11 a) the yield of a chemical reaction is a nonlinear function of the input flow of reactants as shown in Figure 8.11 (b). The reaction we consider here is the conversion of B to C by the input of A in solution (Figure 8.11 a). For a simple isothermal reaction the reaction rate is related to the extent of the reaction as shown in Figure 8.11 (b). Different input flow rates are shown by the red lines. A non-equilibrium stationary state is defined by the intersection of the red flow curves with the black reaction curve. For fast flow rates (curve 1) there is no intersection and so the reaction does not occur. The physical reason for this is that the residence time for A in the reactor is so small the reaction does not have time to occur. For moderate flow rates there

are two intersections (P and Q in Figure 8.11 b). If the reaction rate is faster than the supply of A (corresponding to intersection Q) then ultimately the reaction stops as A is used up. As A then increases in concentration the reaction begins again and speeds up until the supply of A is again exhausted; the process repeats. Thus C is produced in an oscillatory manner. This type of oscillatory stationary state is said to be unstable; another mode of evolution is for the system to switch to P. If the reaction rate is slower than the supply of A (corresponding to intersection P) the reaction proceeds in a stable (non-oscillatory) manner at high yield.

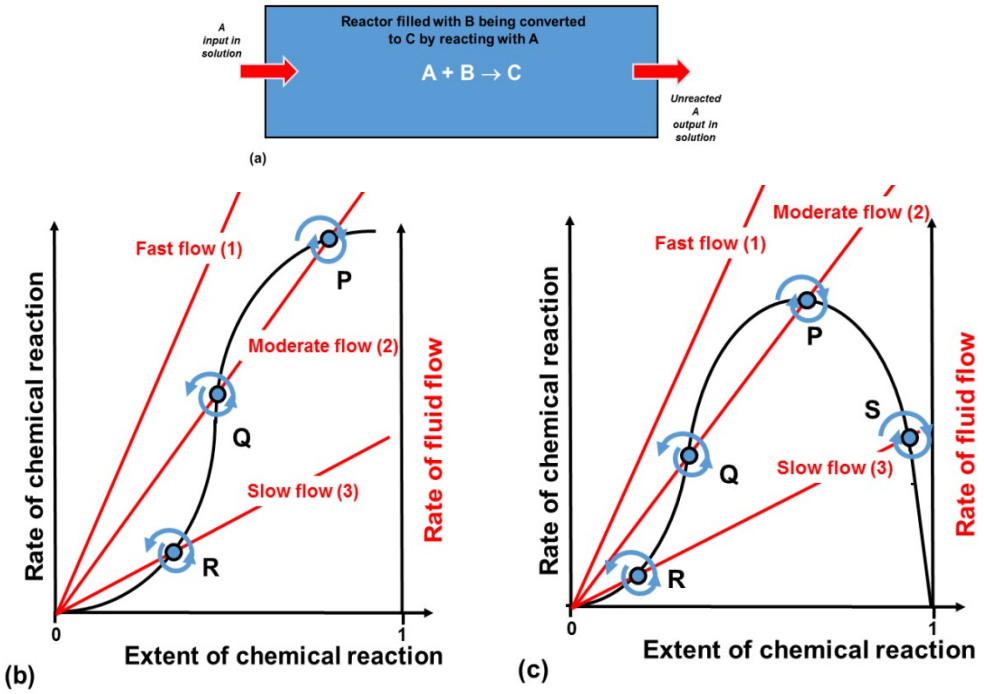

Figure 8.11. The behaviour of chemical reactions in a flow controlled system. (a) An open flow controlled reactor in which B is converted to C by reacting with A in solution. (b) A simple isothermal reaction with the rate of chemical reaction plotted against the extent of the reaction in the black line. Three flow regimes are shown for the input of A. Stationary states are defined by the intersection of the flow curve with the reaction curve. For fast flow rates (1) there is no reaction since the residence time for A is too small for the reaction to ignite. For moderate flow rates (2) there are two intersections, P and Q. These correspond to non-equilibrium stationary states with a high yield for P and a lower yield for Q. We will see that P is a stable stationary state whereas Q is unstable. For slow flows (3) there is one (unstable) intersection, R, at low yield since the reaction rate is small. The chemical engineer needs to adjust the flow rate to generate the highest possible yield for the imposed conditions. (c) The equivalent of (b) for an exothermic reaction. An extra stable stationary state, S, for slow flows is added with a high extent of reaction.

All reactions are governed by the principles outlined in Figure 8.11. Variations on this theme are introduced if the reaction is exothermic as shown in Figure 8.11 (c) for now the relation between reaction rate and reaction extent is a different shape. Further complications arise if there are several coupled chemical reactions occurring simultaneously for now there is competition for supply of nutrients from the coupled processes. If one reaction is exothermic and the other is endothermic then these reactions compete for the supply of heat as well as for the supply of nutrients. In these cases where more than two processes compete the reaction rates can become chaotic rather than oscillatory. Again, if the molar volume of the product is larger than that of the reactant then pore space may be clogged and the reaction ceases. If the molar volume of the product is smaller than that of the reactant then pore space may be locally enlarged resulting in locally faster flow rates so that what was a stable reaction may locally become unstable. Needless to say, all these possibilities can result in a complex response but one should remember that the basic principles are contained in Figure

8.11. It is the task of the chemical engineer to tune these competing processes so as to optimise the yield of the reactor. Mother Nature achieves such tuning when a giant high grade mineral deposit forms.

8.2.3. Governing equations.

The equations governing the behaviour of a reactor are of the form

- Mass balance.
- Heat transfer.
- Fluid transport including the coupled mechanics of permeability generation and destruction.
- Chemical reaction kinetics including the *chemical* mechanisms of permeability generation and destruction.
- Mechanical deformation including the *mechanical* mechanisms of permeability generation and destruction.

There are many examples of equations that have been written to describe the behaviour of chemical reactions including Aris (1961, 1978), Lynch et al. (1982), Gray and Scott (1994), Epstein and Pojman (1998) and Berezowski (2014 and references therein). We consider a very simple reactor where two reactants, A and B, form products C and D according to $\mathrm{A} \xrightarrow[E_1]{k_1} \mathrm{C}$ and $\mathrm{B} \xrightarrow[E_2]{k_2} \mathrm{D}$ where k_1, k_2 and E_1, E_2 are the reaction constants and activation energies of the two reactions. Both reactions are assumed to be exothermic and follow first order Arrhenius rate laws. The mass balance relations are of the form

$$\begin{bmatrix} Rate\ of\ change\ of \\ number\ of\ moles\ of \\ A\ in\ the\ reactor \end{bmatrix} = \begin{bmatrix} Rate\ of\ addition \\ of\ A\ to\ the \\ reactor \end{bmatrix} - \begin{bmatrix} Rate\ of\ removal \\ of\ A\ from\ the \\ reactor \end{bmatrix} + \begin{bmatrix} Rate\ of \\ production\ of \\ A\ in\ the\ reactor \end{bmatrix}$$

For these reactions Lynch et al. (1982) write the mass balance relations in the form

$$\mathrm{V}\frac{d[A]}{dt} = Q([A_0]-[A]) - \mathrm{V}[A]k_1 \exp\left(-\frac{E_1}{R\mathrm{T}}\right) \qquad (8.5)$$

$$\mathrm{V}\frac{d[B]}{dt} = Q([B_0]-[B]) - \mathrm{V}[B]k_2 \exp\left(-\frac{E_2}{R\mathrm{T}}\right) \qquad (8.6)$$

where V is the volume of the reactor, R is the gas constant, Q is the volumetric entrance flow rate and $[A_0]$, $[A]$ and $[B_0]$, $[B]$ are the feed concentrations and local concentrations of A and B. t is time.

The energy balance of the reactor is expressed as

$$\begin{bmatrix} Rate\ of\ change \\ of\ energy\ of \\ the\ reactor \end{bmatrix} = \begin{bmatrix} Rate\ of\ energy \\ released\ by \\ reactions \end{bmatrix} - \begin{bmatrix} Rate\ of\ energy \\ added\ in\ the \\ flow \end{bmatrix} + \begin{bmatrix} Rate\ of\ energy \\ extraction\ in \\ the\ flow \end{bmatrix} - \begin{bmatrix} Rate\ of\ energy \\ removed\ by \\ heat\ transfer \end{bmatrix}$$

which Lynch et al. (1982) write as

$$\mathrm{V}\rho \mathrm{c_P}\frac{d\mathrm{T}}{dt} = H_{r_1}\mathrm{V}[A]k_1 \exp\left(-\frac{E_1}{R\mathrm{T}}\right) + H_{r_2}\mathrm{V}[B]k_2 \exp\left(-\frac{E_2}{R\mathrm{T}}\right) - Q\rho \mathrm{c_P}(\mathrm{T}-\mathrm{T_0}) - SU(\mathrm{T}-\mathrm{T_0}) \quad (8.7)$$

where $\mathrm{T_0}$, T are the feed and reactor temperatures, ρ is the density, $\mathrm{c_P}$ is the isobaric specific heat, H_{r_1}, H_{r_2} are the heats of reaction for reactions 1 and 2, S is the surface area of the reactor where heat is lost and U is the reactor heat transfer coefficient.

Lynch et al. (1982) show that the system of equations (8.5), (8.6) and (8.7) display a range of oscillatory behaviours depending on the ratios $\beta = \frac{H_{r_1}}{H_{r_2}}$ and the Damköhler Number, $\frac{\mathrm{V}}{Q} k_1 \exp\left(-\frac{E_1}{R\mathrm{T}}\right)$. Moreover, since there are three differential equations involved, the system can show chaotic behaviour depending on both β and the ratio, $\frac{E_1}{E_2}$. The attractors derived from these equations (Figure 8.12) resemble classical attractors discussed by Sprott (2003) and Beck and Schlögl (1993) where multifractal geometries are documented.

The reactor described by (8.5), (8.6) and (8.7) is the simplest reactor one can consider where the reactions are coupled only by temperature. More complicated versions where the reactions are coupled by mass transfer and the reactions are autocatalytic are considered by Gray and Scott (1994). Coupled exothermic/endothermic reactions are considered by Kalhert et al. (1981). If reaction-diffusion reactions are included (Epstein and Pojman, 1998), spatio-temporal chaos arises. Many examples of chaotic behaviour in coupled reactors (Figure 8.13) are considered by Berezowski (2014, and references therein). Deformation is not included in any of the classical treatments of chemical reactors. Deformation is responsible for evolution of fluid pore pressure and of permeability and adds yet other sets of equations ensuring that chaos is an essential ingredient in the evolution of the reactor (Section 8.5).

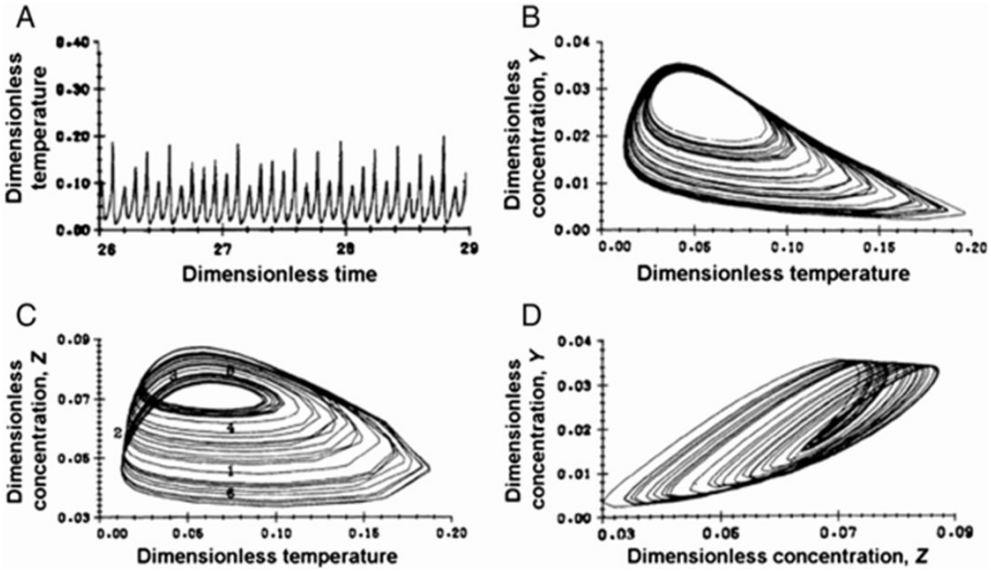

Figure 8.12. Chaotic behaviour of two parallel first order exothermic reactions (after Lynch et al., 1982). (A) Dimensionless temperature plotted against time. (B) Dimensionless concentration Y plotted against dimensionless temperature. (C) Dimensionless concentration Z plotted against dimensionless temperature. (D) Dimensionless concentration Y plotted against dimensionless concentration, Z. The reactions involved here are A → C and B → D, both exothermic. If the concentrations of A and B are a and b with initial concentrations equal to a_0 and b_0 then $Y = a/a_0$ and $Z = b/b_0$.

As a final illustration of the chaotic behaviour of a reactor system we take the case of a reactor (reactor 2 in Figure 8.13 a) that is fed by two streams. One is the primary hydrothermal stream and the other is the output from a neighbouring reactor (reactor 1 in Figure 8.13 a). Examples of this kind of geometry can be found in Figure 8.2. The reaction in

both reactors is A → B. The parameter space we explore is shown in Figure 8.13 (b) and consists of the reaction extent, ξ, the reactor temperature, T, and the temperature of the wall rocks, T_H. Both T and T_H are normalised by the relation

$$T = \frac{\hat{T} - T_0}{\beta T_0}$$

where β is a dimensionless number related to the adiabatic temperature increase and $\hat{T}$ is the physical temperature. T_o is a reference temperature.

The plot of T agains T_H (Figure 8.13 c) shows that as the country rock temperature approaches the reference temperature the system switches from a standard S-curve behaviour to chaotic behaviour and then finally switches to periodic behaviour with bursts of chaos. We show three sections across this diagram in the ξ - T plane in Figures 8.13 (d, e, f). Figure 8.13 (D) corresponds to section A in Figure 8.13 (c) and consists of chaotic behaviour with well defined orbits. A slight change in wall rock temperature leads to increased chaos in Figure 8.13 (e) corresponding to Section B; the attractor in (e) occupies much the same phase space as in (d). Another small change in wall rock temperature leads to periodic behaviour as shown in Figure 8.13 (f) corresponding to Section C. Thus we can expect adjacent ore bodies to be quite different in the extent of reaction (and hence grade) depending solely on slight fluctuations in wall rock temperature.

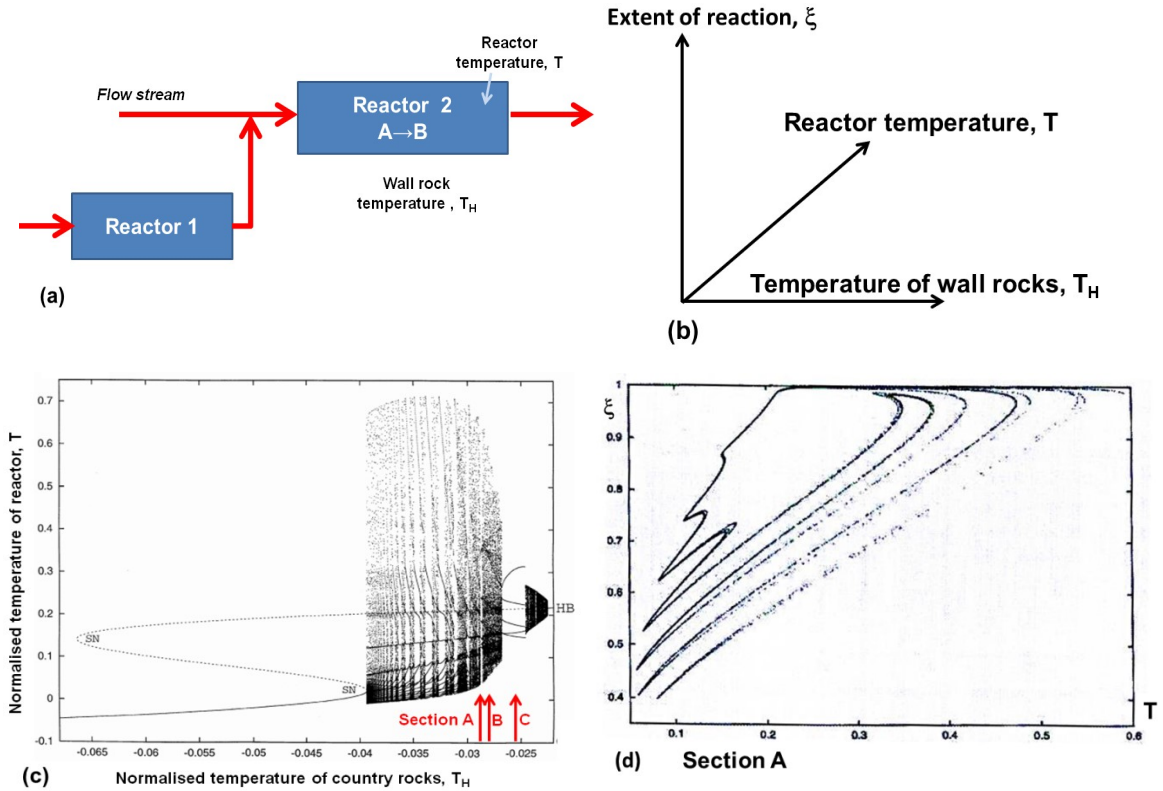

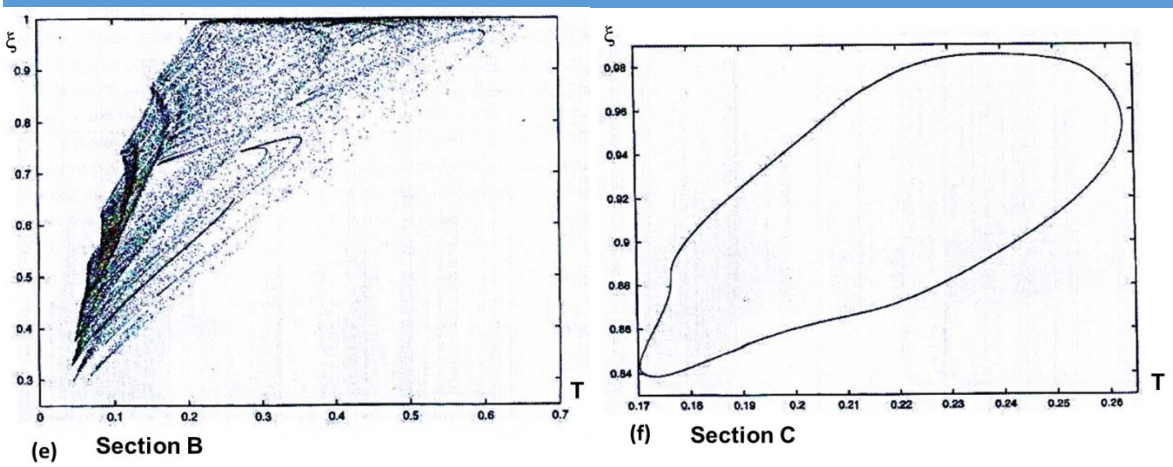

Figure 8.13. Behaviour of a reactor that is fed from two sources. (a) Reactor 2 is fed by the main input stream and from the exhaust from reactor 1. The chemical reaction in reactor 2 is A → B and A is in both input streams. The reaction extent-reactor temperature-wall rock temperature phase space in which the behaviour of reactor 2 is described. (c) A section in reaction temperature-wall rock temperature space showing the transition from S-curve type behavior with static bifurcations, SN, to chaotic behaviour to a window of periodic behaviour to damped oscillatory behaviour ending at a Hopf bifurcation, HB. (d) A section in reaction extent-reactor temperature space at position A in (c). (e) A section in reaction extent-reactor temperature space at position B in (c). (f) A section in reaction extent-reactor temperature space at position C in (c). Adapted from Berezowski (2014).

8.3. Some more detail.

It is instructive to derive some of the relations that describe the operation of chemical reactors to appreciate the simple origins of the complexity that arises. In the following we explore three different reactions each with slightly increased complexity in the type of reaction or nature of the feed to the system. The first is an autocatalytic system involving two minerals A and B but with only A in the feed stream (Figure 8.14 a). The second is the same reaction but with B breaking down to form another mineral, C (Figure 8.14 b). The third is the same reaction again but with both A and B entering in the feed stream (Figure 8.14 c). Although the final set of reactions we consider are still relatively simple they contain all of the features that are combined in various manners in the behaviour of very complicated systems with many coupled chemical reactions.

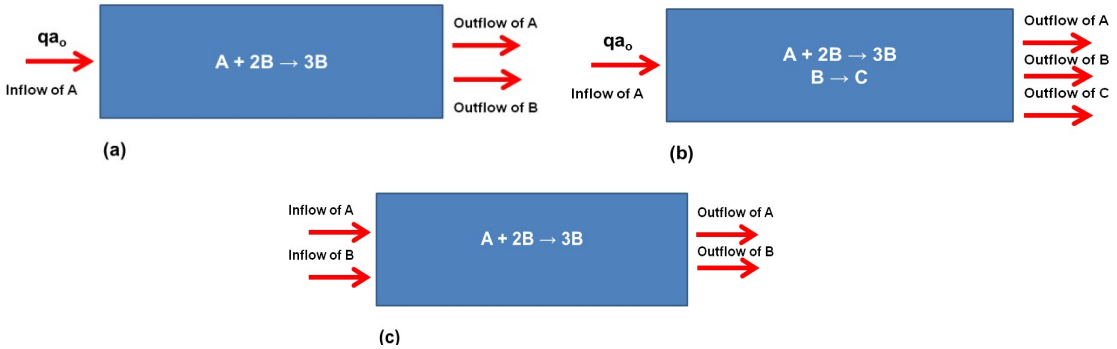

Figure 8.14. Simple reactor systems used as examples. (a) Autocatalysis with only A entering system. (b) Autocatalysis with B decaying to C; only A enters system. (c) Autocatalysis with no decay of B; both A and B enter system.

8.3.1 Cubic autocatalysis with only A entering the system.

In order to show that one uncoupled isothermal chemical reaction can become unstable due to coupling with fluid flow in an open flow system we consider the cubic autocatalytic reaction:

$$A + 2B \xrightarrow{k_1} 3B, \quad \dot{\xi} = k_1 a b^2 \qquad (8.8)$$

The system consists of a flow controlled reactor as shown in Figure 8.14 (a) where a fluid containing A is mixed with B within the reactor and the outflow is the product of the reaction. We concentrate the discussion on the evolution of A. The initial concentration of A in the inflow stream is a_o; there is no inflow of B which has an initial concentration of b_o within the reactor. ϕ is the (assumed homogeneous) porosity of the system.

The concentration of A within the reactor, a, is determined by three quantities: (i) The inflow rate of A: $r_{in} = q\phi a_o$, where q is the volumetric in-flow rate. (ii) The outflow rate of A: $r_{out} = q\phi a$. (iii) The total rate of conversion of A to B: $r_{chem} = Vk_1 a b^2$. Thus,

$$V\frac{da}{dt} = q\phi a_o - q\phi a - Vk_1 a b^2 \qquad (8.9)$$

The concentrations of A and B are related by $a_o + b_o = a + b$ and so

$$\frac{da}{dt} = k_{flow}\phi(a_o - a) - k_1 a(a_o + b_o - a)^2 \qquad (8.10)$$

where we have written k_{flow} for q/V. The concentration of A now evolves to a stationary state value a_{ss} where the chemical production rate balances the inflow and outflow rates so that $\frac{da}{dt} = 0$ and the system is at a stationary state. This non-equilibrium stationary state can be maintained indefinitely so long as the quantity $k_{flow}\phi a_o$ is maintained as the inflow stream and B is not exhausted. Stationary states in the system can be found as solutions to

$$k_{flow}\phi(a_o - a_{ss}) - k_1 a_{ss}(a_o + b_o - a_{ss})^2 = 0 \qquad (8.11)$$

An instructive way to explore these solutions is the use of a *flow diagram* that plots the two rates, the net inflow rate, and the chemical reaction rate as functions of the extent of the reaction, $\xi = (a_o - a)/a_o$. The net flow rate, v is

$$v = k_{flow}\phi(a_o - a) = k_{flow}\phi a_o \xi \qquad (8.12)$$

and the chemical reaction rate is

$$R = k_1 a(a_o + b_o - a)^2 = k_1 a_0 (1-\xi)(b_o + a_o\xi)^2 \qquad (8.13)$$

Points of intersection of (8.12) and (8.13) on the flow diagram where R = v correspond to solutions to (8.10) and hence are stationary state solutions. Note that in many instances the line defined by (8.12) intersects the curve defined by (8.13) in two points showing that two stationary states exist in addition to another which in this case corresponds to the origin; such systems are said to exhibit *bistability*. Figure 8.16 shows some of these solutions for which bistability exists. Gray and Scott (1994, p 21) show that bistability exists for $a_o > 8b_o$. An interpretation of Figure 8.16 in terms of processes operating within the system is given in Figure 8.17. The important point is that the behaviour of the system depends on the value of $k_{flow}\phi a_o$ (or the slope of the red lines in Figures 8.15 and 8.16) and so for constant fluid flow rate and a given concentration of the reactant A, the behaviour of the

system will vary with the porosity which ultimately is expressed as variations in the permeability.

Gray and Scott (1994, Chapter 6) also consider the influence of adding reversibility and influx of B to reaction (8.8). The basic behaviour remains as described above. Bistability remains as the essential characteristic of the nonlinear behaviour and no oscillatory behaviour emerges.

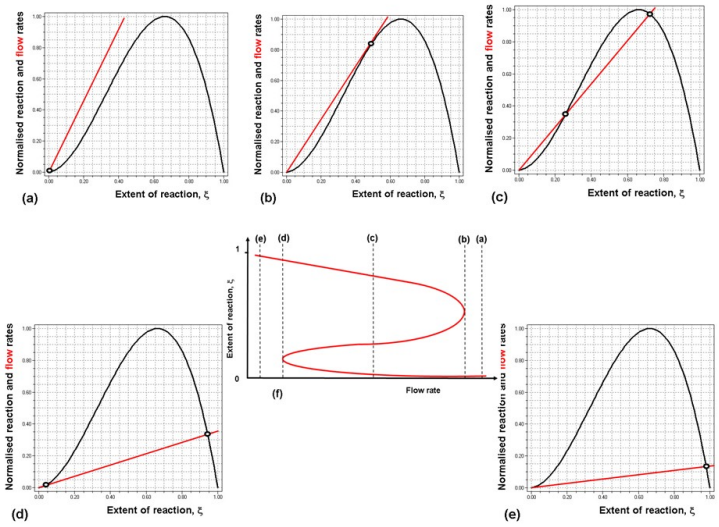

Figure 8.15. Flow diagrams showing the origin of bistability for cubic autocatalysis in an open flow-controlled system. The red line in (a) through to (e) is the net flow rate whilst the black curve is the chemical reaction rate. (f) Stationary states for the cubic autocatalytic reaction with flow. The red line is the plot of extent of reaction against flow rate showing the presence of three stationary states for flow rate conditions between (b) and (d).

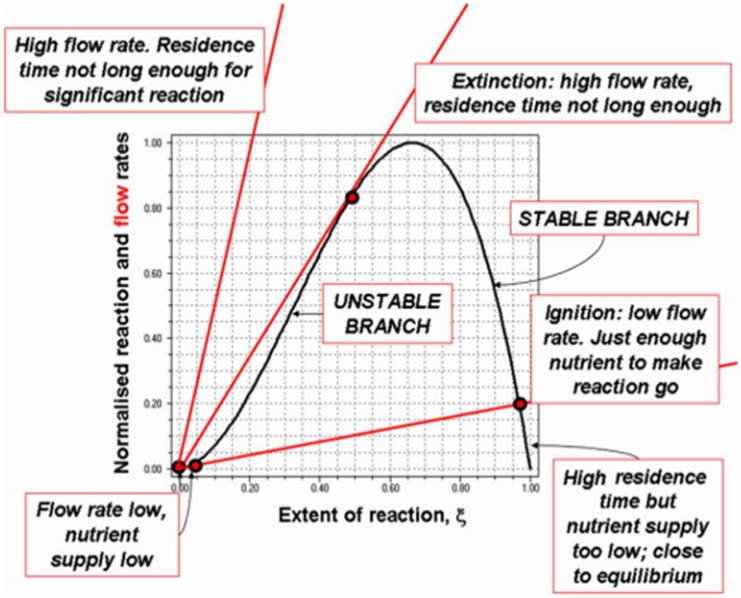

Figure 8.16. Summary diagram showing the behaviour of the cubic autocatalytic reaction (8.8) in a flow controlled system.

8.3.2. Cubic autocatalysis with decay of B.

We now consider a slight change in the flow controlled system where the component B decays to a new product C (Figure 8.14) so that the complete set of reactions is

$$A + 2B \xrightarrow{k_1} 3B, \quad \text{rate} = k_1 a b^2$$

$$B \xrightarrow{k_2} C, \quad \text{rate} = k_2 b \qquad (8.14)$$

Only A is fed to the system but A, B and C are extracted. The initial concentration of C is taken to be zero so that $c = (a_o + b_0) - (a + b)$. The rate equations now become

$$\frac{da}{dt} = q\phi(a_o - a) - k_1 a b^2$$

$$\frac{db}{dt} = q\phi(b_o - b) + k_1 a b^2 - k_2 b \qquad (8.15)$$

We define the dimensionless groups α, β and κ_2 as

$$\alpha = \frac{a}{a_o}, \ \beta = \frac{b}{a_o}, \ \kappa_2 = \frac{k_1}{k_2 a_o^2} \qquad (8.16)$$

The mass balance equations (8.15) become

$$\frac{d\alpha}{dt} = q\phi(1 - \alpha) - \alpha\beta^2$$

$$\frac{d\beta}{dt} = q\phi(\beta_o - \beta) + \alpha\beta^2 - \kappa_2\beta \qquad (8.17)$$

The stationary state concentration β_{ss} is given by

$$\beta_{ss} = \frac{1 + \beta_0 - \alpha_{ss}}{1 + (\kappa_2 / q\phi)} \qquad (8.18)$$

We substitute (8.18) into the equation expressing the stationary state of α: $\frac{d\alpha}{dt} = 0$ to obtain an equation for the stationary state of the system:

Flow rate – **Reaction rate** **= 0**

$$\frac{(1 + \kappa_2 \tau_{res})^2}{\tau_{res}}(1 - \alpha_{ss}) - \alpha_{ss}(1 + \beta_o - \alpha_{ss})^2 = 0 \qquad (8.19)$$

As opposed to the situation where there is no decay of B the flow rate is now a quadratic function of the residence time although still a linear function of the extent of the reaction. This means that the slope of the flow line on a flow diagram is steep at low residence times and decreases initially as the residence time increases. However the slope reaches a minimum at

$$\frac{dv}{d(1 - \alpha_{ss})} = 4\kappa_2 \qquad \text{when } \tau_{res} = \frac{1}{\kappa_2} \qquad (8.20)$$

and then increases again as the residence time increases. If $b_o = 0$ then (8.19) becomes

$$\frac{(1 + \kappa_2 \tau_{res})^2}{\tau_{res}}(1 - \alpha_{ss}) - \alpha_{ss}(1 - \alpha_{ss})^2 = 0 \qquad (8.21)$$

and a plot of extent of reaction ($1-\alpha_{ss}$) against the residence time becomes that shown in Figure 8.17 together with ($1-\alpha_{ss}$) = 0. Instead of the S-shaped curve of Figure 8.15 (f) we now have a closed curve known as an *isola* together with the straight line ($1-\alpha_{ss}$) = 0. In this system it is not possible to have very long residence times that approach complete reaction and hence equilibrium. There is a minimum flow rate corresponding to a finite extent of reaction. This minimum flow rate is given by (8.20) and is a function of the input concentration of A.

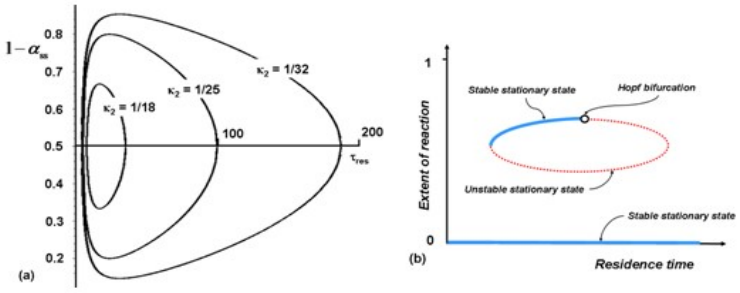

Figure 8.17. An isola as a stationary state locus for reactions with no autocatalytic inflow and $\kappa_2 < 1/16$. (a) Isola for various values of κ_2. In addition the line $1-\alpha_{ss} = 0$ exists as a solution for all conditions. (b) Stability of stationary states. Blue represents stationary steady states, dotted red are unstable stationary states. Open circle is a Hopf bifurcation. See Gray and Scott (1990, Chapter 6) for discussion and details.

Although the stationary states are now defined by (8.19) not all of them are stable. Gray and Scott (1994, Chapter 6) discuss the stability of the system in some detail and show that the lowest branch $\xi = 0$ is always stable as is part of the uppermost branch. However the lowest part of the isola is always unstable together with part of the uppermost branch as shown in Figure 8.14 (b). Moreover the point that marks the loss of stability on the uppermost branch corresponds to a complete change in behaviour of the system. This is known as a *Hopf bifurcation* which represents the appearance or disappearance of periodic behaviour associated with the change in stability (Guckenheimer and Holmes, 1986, Wiggins, 2003). In general a Hopf bifurcation can be supercritical or subcritical. If one plots the behaviour of a system in phase space (a phase portrait) then a supercritical Hopf bifurcation is represented by oscillations of decreasing amplitude that ultimately settle into a limit cycle. The system can also start at a limit cycle and oscillate to a fixed point. A subcritical Hopf bifurcation can begin at a fixed point and oscillate to a limit cycle or start at a limit cycle and evolve with increasing amplitude of oscillations. Both types of behaviour are possible on the uppermost branch of the isola. One type of behaviour is for the system to undergo a Hopf bifurcation which ends on the stable lowermost branch corresponding to $\xi = 0$. Thus the behaviour of this relatively simple system is complex and quite different forms of behaviour emerge with small changes in residence time (and hence of porosity). In this system with constant supply of A, adjacent pieces of rock with slight fluctuations in porosity can have quite contrasted behaviours: one can undergo oscillations of chemical composition at high values of the reaction extent whilst immediately adjacent areas show no reaction at all. This has nothing to do with whether fluid has or has not accessed the relevant parcel of rock; it is controlled solely by the local flow rate and hence the local permeability.

8.3.3. Cubic autocatalysis with A and B entering the system.

The next step in complexity is to add an inflow of concentration of B, that is $b_0 \neq 0$; then the response becomes much more complicated. The gradient of the flow line is still given by the first term in (6.18) but now the reaction rate is a function of β_o. An example of the flow diagram and the resulting stationary state loci are given in Figure 8.18 where both isola and mushrooms (Figures 8.18 f, h) can emerge. As in the case of cubic autocatalysis with $b_o = 0$ (Figures 8.17) not all of the stationary states shown in Figure 8.18 are stable and the unstable behaviour of the system is illustrated in Figure 8.18 where dotted lines show unstable states and black dots show Hopf bifurcations. Again it is clear that slight fluctuations in the flow rate can induce dramatic changes in system behaviour such as the sudden emergence of oscillatory behaviour from a stable stationary state or a sudden drop or increase in reaction extent.

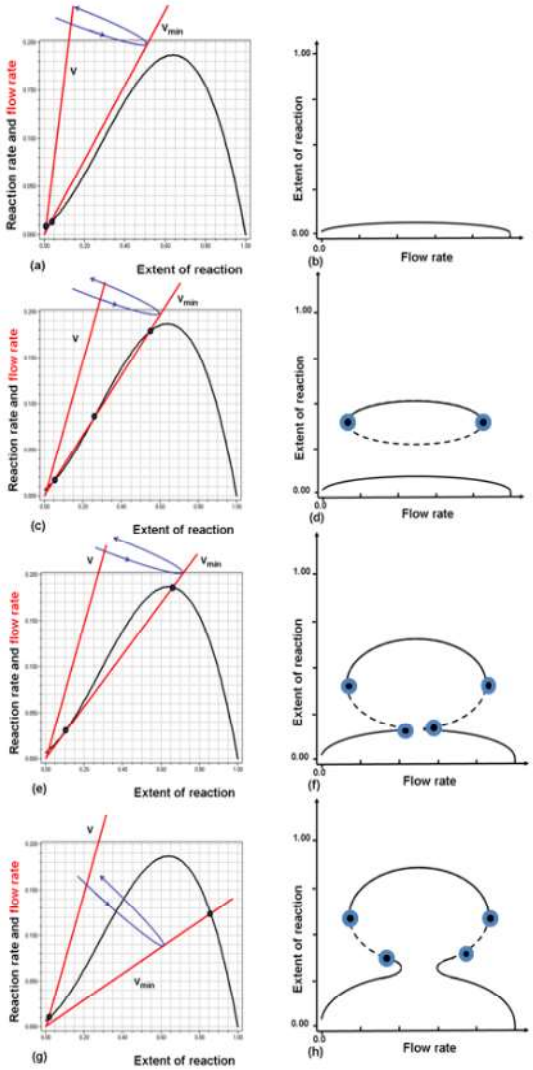

Figure 8.18. Flow diagrams representing different stationary states for cubic autocatalysis with inflow and decay of B. (a) and (b) Single stable branch at low values of ξ. (c) and (d) Isola plus lower branch. (e) and (f) Transition from isola to mushroom. (g) and (h) Mushroom. Some unstable branches are shown dotted. Black dots are Hopf bifurcations.

8.4. Aspects of fluid – solid reactions.

Most of what we have discussed above concerning the nonlinear behaviour of chemical systems has been developed for reactions occurring in well mixed fluid systems. Nevertheless the basic principles involved apply to fluid- or gas-solid systems although the

details of the processes involved are generally more complicated. Such details involve the dependence of reaction rates on particle size, the control of fluid pressure variations by particle size, the clogging of porosity by mineral deposition (and hence poor reactor yield) and by trapping of particles during fluid transport, the generation of connected porosity by dissolution during chemical reactions and the disaggregation (brecciation) of solids by chemical processes. In addition many of the chemical reactions now involve processes operating at fluid/solid interfaces and an array of coupled processes arise involving competition in reaction rates between different reaction sites on the solid surface and the transport of reactants for one site to another in the fluid that are of major importance. Again most of these competitive processes result in oscillatory or chaotic behaviour.

It is clear that any detailed discussion of hydrothermal systems must involve an assessment of the importance of these processes but we defer such an analysis to future publications. We include some reference to such processes in the recommended readings. The basic outcome that concerns us is that the processes commonly involve episodic variations in temperature and fluid pressure and a critical dependence of reaction rate and reaction yield on subtle changes in the rates at which nutrients and heat are supplied to the reaction site. In Chapter 12 we concentrate on one aspect of the processes discussed above, namely oscillatory behaviour and its relevance to gold deposition.

8.5. The generation of heat during deformation of the hydrothermal system: a model for brecciation.

When the temperature of a closed (undrained) porous medium increases the pore pressure increases by an amount that is governed by the difference in thermal expansion of the pore fluid and the solid skeleton. Such increases in pore pressure are of fundamental importance to the behaviour of a hydrothermal system since these changes influence the effective stress and hence whether the system will fail by fracturing, veining or brecciation. The increases in temperature can arise from the heat liberated by exothermic reactions or from the heat generated by deformation (especially frictional sliding on fractures) or by coupled deformation and chemical reaction processes. The purpose of this section is to discuss these processes.

The pore fluid pressure is also influenced by how rapidly pore pressure can diffuse in the system and by the addition of fluid from outside the system (if the system is open) and by the addition of new fluid from devolatilisation reactions within the system. Thus one can write a balance relation that describes how the pore pressure changes with time in a system:

$$\begin{bmatrix} Rate\ of\ change \\ of\ fluid\ pressure \end{bmatrix} = \begin{bmatrix} Rate\ of\ fluid\ pressure\ change \\ arising\ from\ diffusion\ of \\ fluid\ pressure \end{bmatrix} + \begin{bmatrix} Rate\ of\ fluid\ pressure\ change \\ arising\ from\ temperature\ change \end{bmatrix}$$
$$+ \begin{bmatrix} Rate\ of\ fluid\ pressure\ change \\ arising\ from\ devolatilisation \end{bmatrix} + \begin{bmatrix} Rate\ of\ fluid\ pressure\ change \\ arising\ from\ supply\ of\ fluid \\ from\ outside\ the\ system \end{bmatrix} \quad (8.22)$$

Thus the system is described by a somewhat extended reaction diffusion equation comprising a diffusion term and with many contributors to the fluid pressure generation term. Hence we expect the system to show the rich variety of spatial and temporal patterning that reaction-diffusion systems are known to display. The situation is made even more interesting in that, as shown in Figure 8.1, the pore pressure changes can be linked to episodic increases

in temperature and to episodic bursts of devolatilisation so the system has the potential to not only show the spatio-temporal patterning that reaction-diffusion systems typically show but also for the system to be forced by the episodic supply of nutrients and heat.

Clearly such thermo-chemical pore pressure fluctuations are of fundamental importance in hydrothermal systems and have fundamental implications for the origin of three ubiquitous features of hydrothermal mineralising systems.

(i) Crack-seal vein systems.

Episodic increases in pore pressure, even subtle ones, can open and close vein systems with associated episodic deposition of quartz during pressure drops. This is a mechanism for generating crack-seal microstructures.

(ii) Breccias.

If the pore pressure is such that the effective stress exceeds the value where rock breakage occurs then brecciation consisting of *in situ* fragmentation and /or spalling from the walls of conduits propped open by fluid pressure can occur. If the pressure generation is episodic then overprinting cycles of fragmentation, spalling and cementation occur.

(iii) Fluidised breccias.

If the pore pressure exceeds lithostatic then the potential exists to fluidise the system and to support and transport brecciated fragments in fluid transport systems arising from fluid pressure gradients. Again if the fluid pressure gradients are episodic then overprinting cycles of fragmentation, transport and cementation occur.

(iv) The distribution of gold in veins or within wall rocks and the distinction between refractory and non-refractory ores.

The deposition of gold and of quartz in hydrothermal systems is strongly linked to decreases in temperature and/or fluid pressure. These changes may in turn be responsible for changes in pH or Eh and/or be responsible for boiling or phase separation which are also commonly quoted as drivers for gold deposition but the generic reasons for these changes in chemistry or physical state of the fluid system lies in fluctuations in temperature and pressure. If one relies on events external to the hydrothermal system to drive such changes in temperature or fluid pressure then the response times are such as to be too slow to make a difference on the time scale of the system evolution. The mechanisms for producing large fluctuations in fluid pressure and temperature must be local and hence internal to the system and strongly linked to the deformation and chemical reactions occurring in the system. We explore these processes in some detail in Chapter12 but give an indication of the processes involved here.

The nature of gold distribution in hydrothermal systems, whether it be in veins, in wall rocks adjacent to veins, or is free gold (non-refractory) or bound up within arseno-pyrite grains (refractory) is intimately related to the competition between process expressed in (8.22) and the processes controlling the timing of grain growth of pyrite or of arseno-pyrite relative to that of deposition of gold (Figure 8.19). In this section we discuss the episodic evolution of temperature and pore pressure that arise from the competition between terms in (8.22). If pyrite grows during the part of the cycle where both temperature and pressure are rising then gold is incorporated into the growing pyrite. Such a reaction might be

$$3\text{Chlorite} \Rightarrow 2\text{Muscovite} + 15\text{Pyrite} + 3\text{Quartz}$$

If the pyrite grows during the relaxation phase of the cycle then free gold forms. This is typified by the reaction

$$AuHS_2^- + Fe^{2+} \rightarrow Au + FeS_2 + 0.5O_2$$

Thus a detailed understanding of the mineral reactions involved in the formation of pyrite and where these reactions sit with respect to the episodic evolution of temperature and pore pressure is essential to understanding whether gold will be in "free" form or "invisible".

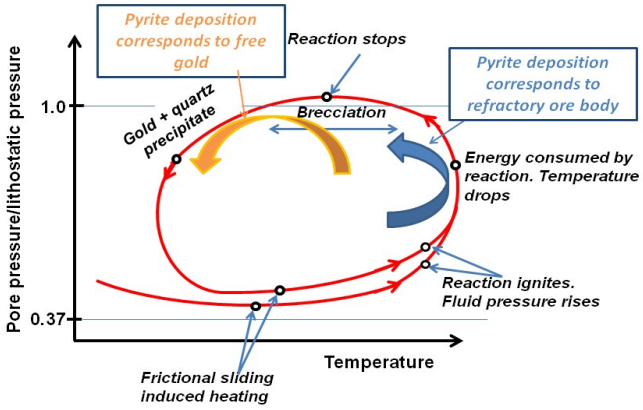

Figure 8.18. Processes that lead to refractory and non-refractory ore bodies.

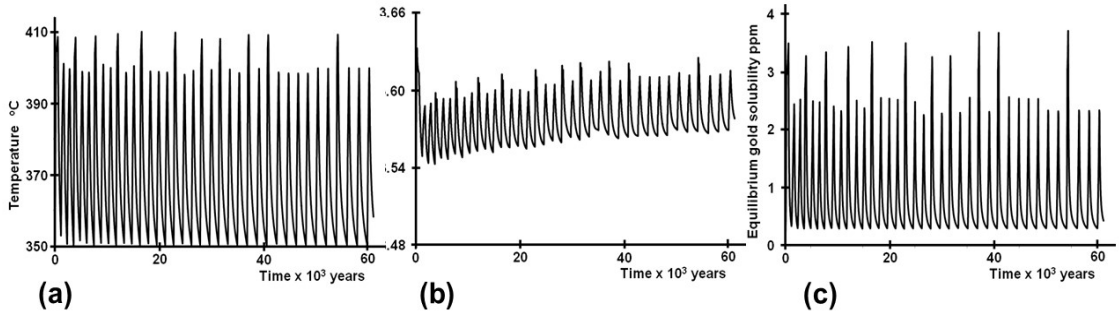

Figure 8.19. Episodic behaviour of a system in which deformation is coupled with an endothermic mineral reaction that liberates fluids. Details of such models are presented in Chapter 12. (a) Temperature history over 60,000 years. (b) Fluid pressure history. (c) Equilibrium gold solubility history.

In the following we develop a nonlinear model for breccia formation with links to the mechanisms of quartz and gold deposition. One of the characteristics of breccia formation is the occurrence of multiple overprinting events. In many instances each event is associated with precipitation of quartz or carbonates or other materials that cement the breccia and this cement is itself overprinted by other brecciation and cementation phases. Gold or sulphides are clearly associated with many breccias and they do not form a relationship that is clearly linked with the cementation events. The model we develop explains all these features.

Figure 8.20. Brecciated material incorporated in a carbonate vein. Sunrise Dam deposit, Western Australia. The fragments have spalled off the walls during a period when pore fluid pressure was close to hydrostatic because of low temperatures in the fluid.

We begin with a body of rock that has already been hydrothermally altered to an assemblage containing hydrous minerals such as kaolinite or chlorite. In some instances such assemblages may even be part of an early regional metamorphic event. For simplicity we

assume the rock mass is subjected on its boundaries to a normal stress, σ_N, and a shear stress, τ_N, as shown in Figure 8.21. The thickness of the system is d and a temperature distribution is developed such that the temperature at the central line of the system is T_{core}. The rock mass deforms by frictional sliding on pre-existing and newly developed fractures with a constitutive law that depends on pressure and is thermally activated through an Arrhenius term. Heat is generated and diffuses from the system by frictional sliding; q_f is the heat flux arising from frictional sliding and that from chemical reactions is q_h. The mode of deformation is by fracturing of grains and subsequent sliding on these fractures. The system is subjected to a fluid Darcy flux, $\hat{V}$. As the system deforms, heat is generated by frictional sliding and chemical reactions proceed within the system comprised of dehydration of the initial hydrous assemblage and precipitation of quartz as a cement and gold.

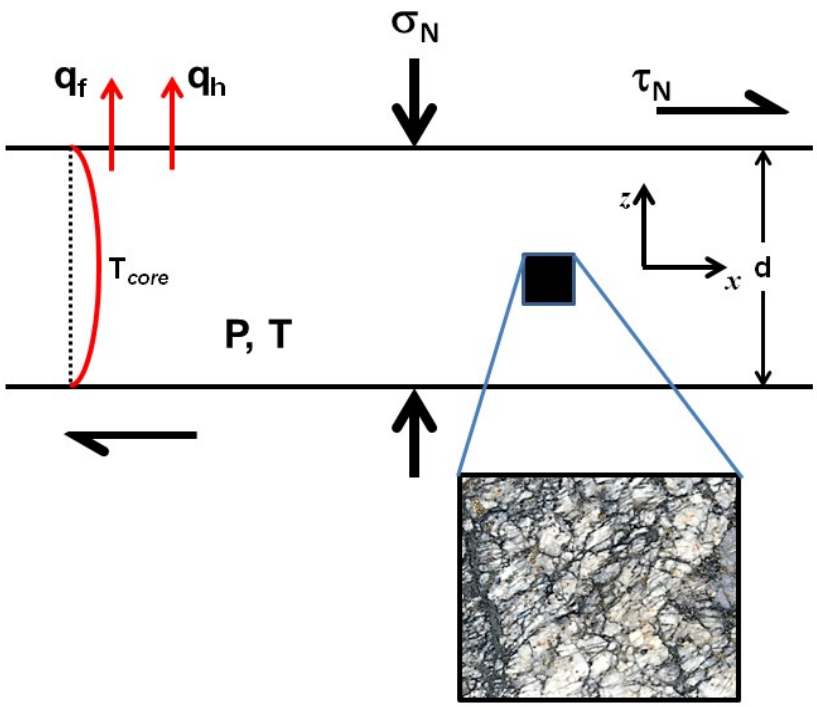

Figure 8.21. A model for brecciation. A system of thickness, d, and core temperature, T_{core}, is deformed by a shear stress, τ_N, and normal stress, σ_N. The ambient temperature and pressure is T and P. Heat is generated by the deformation (frictional sliding on fractures) and leaves the system via the flux, q_f. Other heat sources/sinks arising from chemical reactions are associated with a heat flux, q_h. The result is a crackle breccia shown as inset arising from the increase in pore fluid pressure generated by the heat from frictional sliding. The resultant change in effective stress causes brecciation.

The behaviour of the system is characterised by a set of four dimensionless numbers, namely, the Gruntfest number, *Gr*, the Lewis number, *Le*, the Arrhenius number, *Ar*, and the Damköhler number, *Da*.

The Gruntfest number is the ratio of the ratio of the characteristic time for heat transfer to the characteristic time for energy transfer; such energy arises in this model from the heat released or absorbed by chemical reactions. *Gr* is given by

$$Gr = \frac{\beta_T \tau_N \dot{\gamma}_0}{k_F |\Delta H| \rho_{AB}}$$

where $\dot{\gamma}_0$ is the shearing strain rate, β_T is the Taylor-Quinney coefficient that measures the amount of heat arising from deformation that is stored in the material and available to drive

other processes such as chemical reactions , k_F is the thermal conductivity of the fluid, ρ_{AB} is the density of the solid AB that reacts to form A_{solid} and B_{fluid}, and $|\Delta H|$ is the magnitude of the heat of reaction associated with the reaction $(AB)_{solid} \rightarrow A_{solid} + B_{fluid}$.

In the process we consider here heat is produced by friction and breakage whilst this heat is lost by absorption in endothermic reactions and by thermal diffusion. When $Gr \rightarrow 0$ the heat produced by friction and breakage can be absorbed by the system. When $Gr \rightarrow \infty$ the heat produced by friction and breakage is large and can be used to drive endothermic reactions. Thus at small values of *Gr* the system is characterised by frictional and breakage behaviour whilst at large values of *Gr* the system is characterised by the behaviour of the chemical reactions.

The Lewis number is the ratio of the diffusivity of heat to the diffusivity of mass. *Le* varies with temperature and pore pressure. *Le* is given by

$$Le = \frac{\kappa_M \mu_f \left(\beta_f + \beta_s\right)}{k_\pi}$$

where κ_M, μ_f, β_f, β_s, k_π. If the permeability varies between 10^{-21} m^2 and 10^{-14} $m^{2,}$, then $10^{-3} \le Le \le 10^3$ where the low permeability corresponds to a large value of *Le*.

The Arrhenius number is the ratio of the activation energy for a process or chemical reaction, E_F, to R times a reference temperature, T_c, where R is the gas constant. Thus *Ar* is given by

$$Ar = \frac{E_F}{RT_c}$$

Since activation energies for geologically interesting processes and reactions vary between 40 KJ mol^{-1} and 500 KJ mol^{-1} and such processes are triggered at temperatures from 100°C to 1200°C, *Ar* can take values between 10 and 150. For calcite decomposition, E_F = 200 KJ mol^{-1} at 600°C so that the corresponding value of *Ar* is ≈ 40.

The Damköhler number is the ratio of the chemical time scale (the reaction rate) to the advective mass transport rate. For a reaction A → B of order N with rate constant *k*, in a system with residence time τ, *Da* is given by

$$Da = k a_0^{N-1} \tau$$

The processes that operate in this system are as follows:

(i) Sliding on fractures generates heat which is lost to the system at first by conduction and advection in the moving fluid. The response of the system at this stage is represented by the dashed line ABE in Figure 8.22 which is a plot of the core temperature of the shearing zone against the Gruntfest number. As with many of the chemical reaction systems we have examined in this Chapter the response is multi-valued.

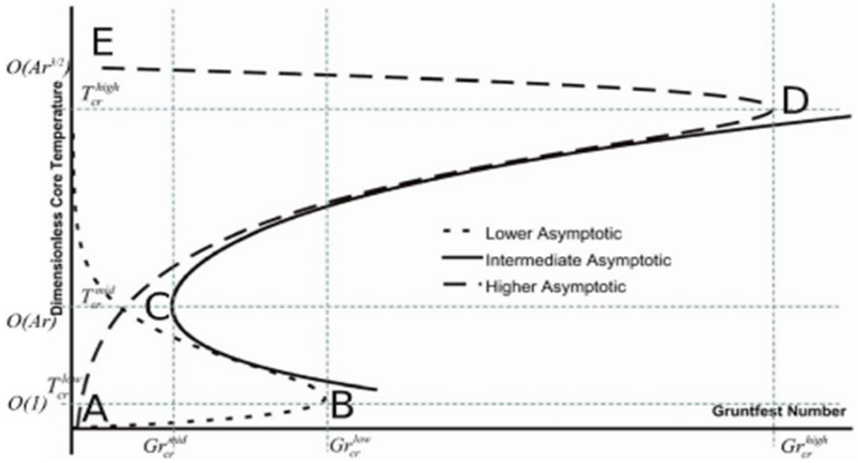

Figure 8.22. Qualitative representation of the behaviour of the system. At low values of *Gr* and low dimensionless temperatures the system is dominated by frictional heating and described by the curve ABE. At larger values of *Gr* and at higher dimensionless temperatures the system is dominated by chemical heating and described by the curve ADE. The two curves cross at C.

The types of chemical reactions that might take place here are typified by

$$3Al_2Si_4(OH)_2 + K_2O \rightarrow 2KAl_3Si_3O_{10}(OH)_2 + H_2O + 6SiO_2$$

Pyrophyllite *Muscovite* *Quartz*

Or,

$$KFe_3^{2+}AlSi_3O_{10}(OH)_2 + 0.5O_2 \rightarrow KAlSi_3O_8 + Fe_3O_4 + H_2O$$

Annite *K-feldspar* *Magneite*

Or,

$$KFe_3^{2+}AlSi_3O_{10}(OH)_2 + Fe_3O_4 + 3S_2 \rightarrow KAlSi_3O_8 + 6FeS + H_2O + 3.5O_2$$

Annite *Magneite* *K-feldspar* *Pyrrhotite*

These reactions are representative of reactions involving the dehydration of hydrous alteration phases. Similarly we can consider the decarbonation of alteration phases such as siderite and ankerite that contain CO_2.

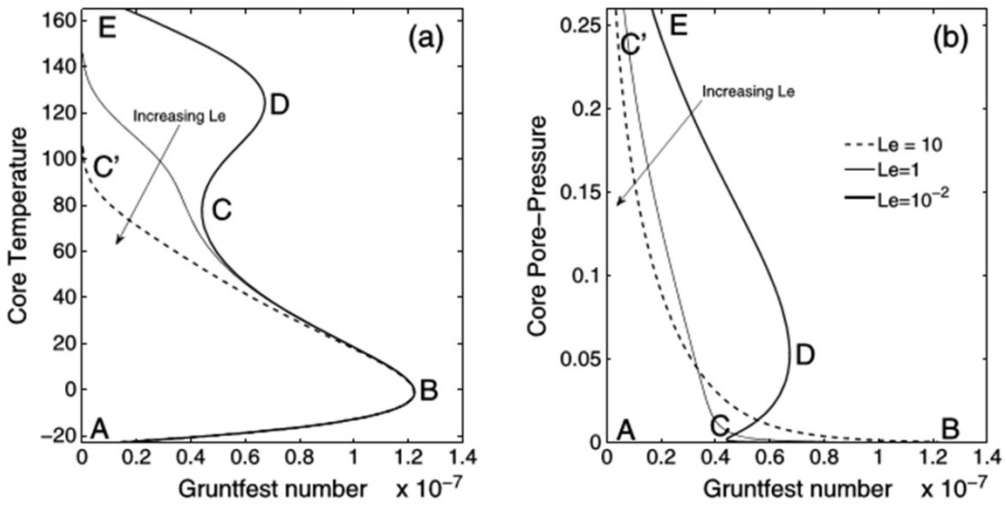

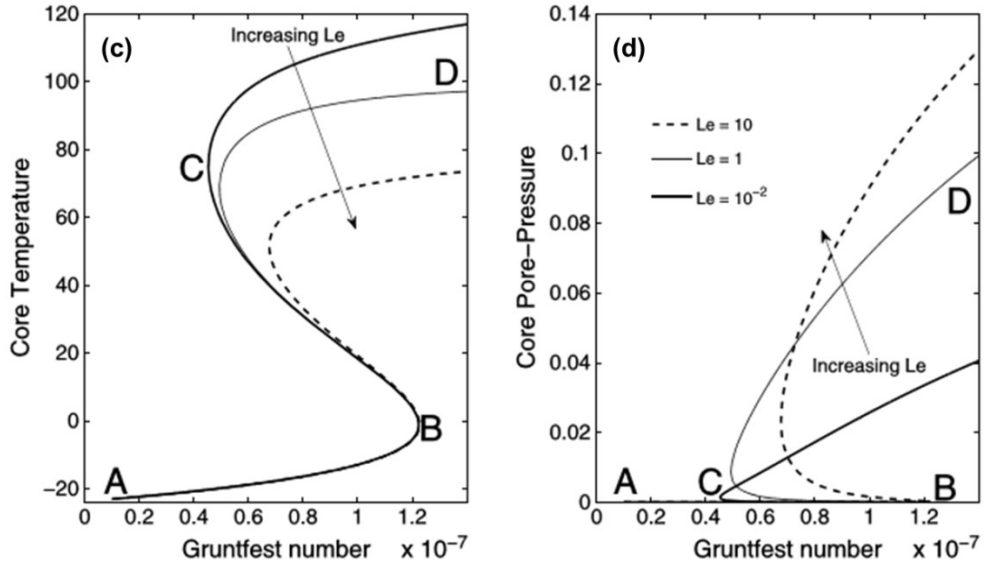

Figure 8.23. Response curves for various values of the Lewis number. Le. High values of Le correspond to low perameabilities and *vice versa*. (a) and (b) correspond to the thermal softening case whereas (c) and (d) correspond to thermal hardening. The letters A, B, C, D, E correspond to the same positions in Figure 8.24. (a) and (c) are plots of core temperature against Gr. (b) and (d) are plots of core pore pressure against Gr. (From Alevizos et al., 2014).

The behaviour of the system is represented in figures 8.24 and 8.25.

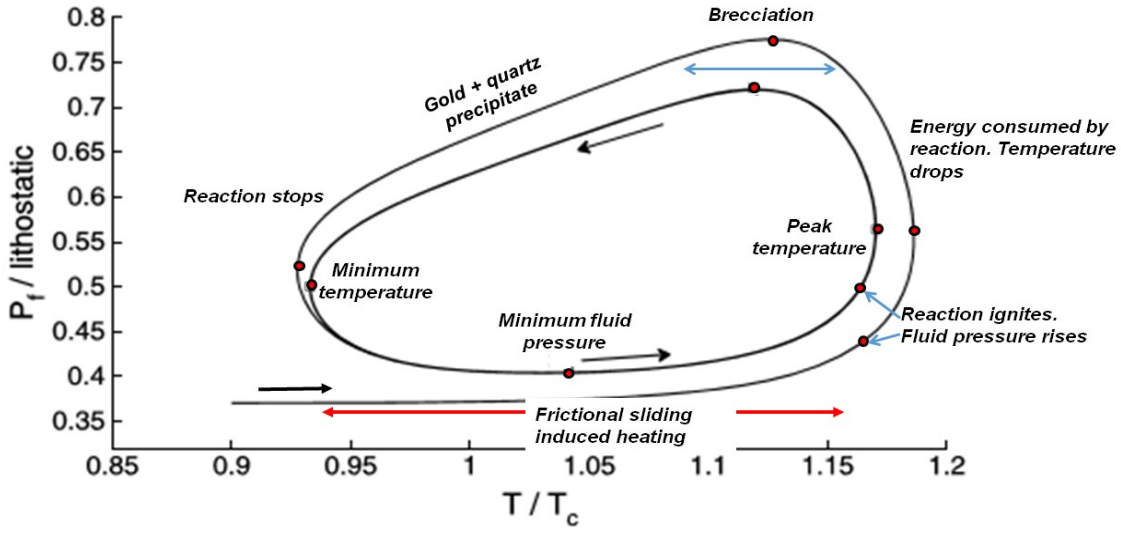

Figure 8.24. The brecciation cycle in pore pressure/temperature space.

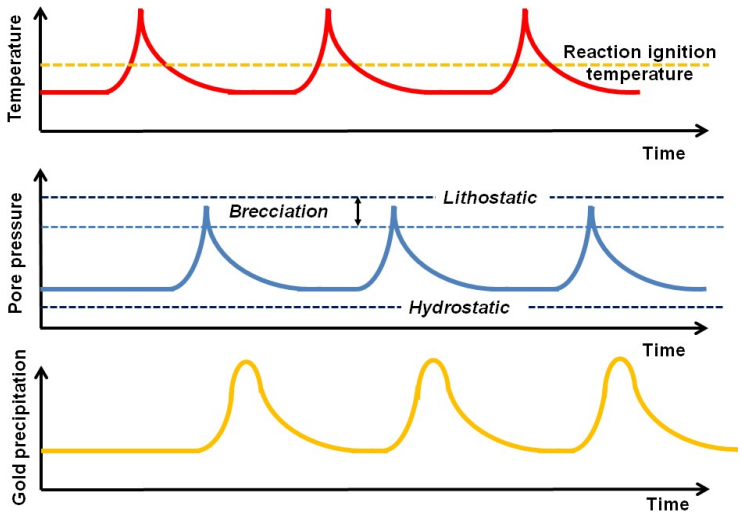

Figure 8. 25. Episodic behaviour arising from Figure 8.24. Top panel: episodic temperature arising from frictional sliding on fractures. This gives rise to episodic pore pressure fluctuations that are out of phase with the temperature fluctuations (middle panel). Gold deposition occurs due to both temperature and pressure decreases. The gold deposition process is smeared over the relaxation parts of the temperature/pore pressure cycles.

8.6. The formation of hydrothermal vein systems.

The coupling between mineral reactions that involve a volume change and fluid flow results in behaviour fundamental to the operation of hydrothermal systems. In particular the behaviour of any system that involves compaction and fluid flow is unstable with respect to small perturbations in fluid pressure away from a homogeneous state; the perturbations grow exponentially and result in pattern formation; the system switches from homogeneous to patterned regions of compaction, where fluid is expelled, and regions of expansion where fluid is absorbed. The instability results from competition between the rate of compaction and the rate at which fluid can diffuse through the material. The patterns take on many shapes including bands (or layers), square checkerboards and hexagonal arrays. The physics of this process is identical to that described by Biot under the title of *internal buckling*. In systems where compaction arises from grain crushing these patterns are called compaction bands but the process is more general and applies equally to devolatilisation reactions where there is a net volume compaction and fluid diffuses from the compacted region carrying dissolved material in the form of $Si(OH)_4$ or $Ca(COH)_3$.

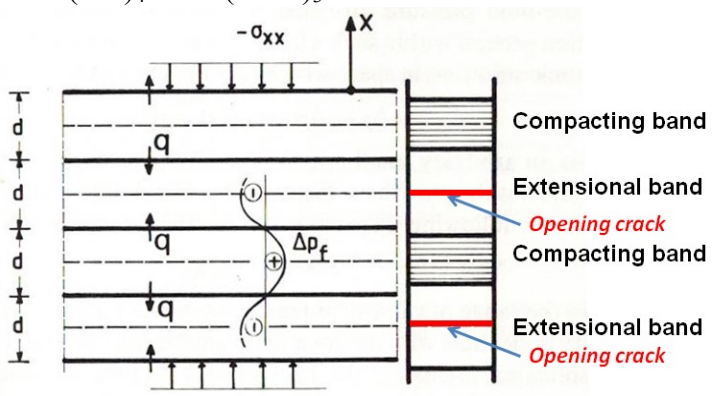

Figure 8.26. The geometry of compaction and extensional banding in a saturated compacting porous medium. A fluid saturated porous medium undergoing compaction due to a stress σ_{xx} is unstable and splits into alternating compacting and extending bands. The pore pressure adopts a sinusoidal distribution so that fluid is expelled from the compacting zones and flows into the extending zones. We envisage the compacting zones to be collapsing chemically due to an alteration reaction such as one described in Table 8.2. The extension is such that

a crack nucleates in the extending band and this ultimately grows to form a vein, utilising the dissolved material in the fluid expelled from the compacting band. Modified from Vardoulakis and Sulem (1995, figure 5.8.5).

As an indication of the compaction magnitudes involved some typical alteration reactions are shown in Table 8.2. Only solid products are included so that some reactions also involve the production of H_2O and/or CO_2. Modest compaction strains are involved for some but if material such as SiO_2 and calcite/dolomite are removed in solution then very large compaction stains are possible for most reactions.

Table 8.2. Volume changes associated with alteration reactions. Modified after Booden and Mauk (2011).

Reaction	ΔV% (with quartz)	ΔV% (with all quartz removed)	ΔV% (with all quartz + carbonate removed)
3Albite → Muscovite + 6Quartz	-7.7	-53.4	
Albite → Adularia	+8.9	-	
5Diopside + 2Albite → Chlorite + 13Quartz	-4.6	-60.3	
5Enstatite + 4Albite → 2Chlorite + 16Quartz	+10.2	-40.9	
Titanite → Calcite +Rutile + Quartz	+40.9	+0.1	-66.2
3Tremolite + 2Epidote → 3Chlorite + 10Calcite + 21Quartz	+36.7	-8.7	-42.2
3Chlorite → 2Muscovite + 15Pyrite + 3Quartz	+10.9	+1.0	
3Chlorite + 15Calcite → 2Paragonite + 15Dolomite + 3Quartz	+9.4	+3.5	-77.8

When the regions of compaction are arranged in layers and the extensional strains in the regions between the compaction layers results in stresses that exceed the fracture strength of the material then planar fractures develop and dissolved minerals from the adjacent reaction are deposited in the fracture. If the reaction proceeds in an episodic manner then crack-seal microstructures develop (Figure 8.27).

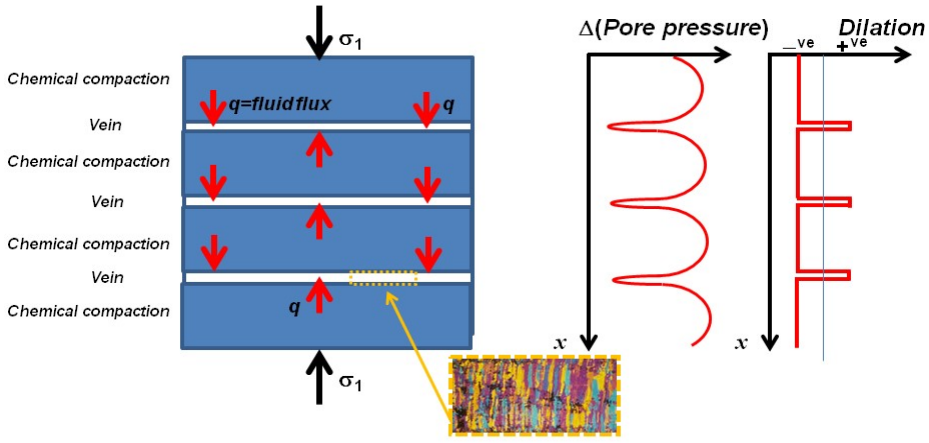

Figure 8.27. The formation of hydrothermal crack-seal veins by chemical compaction. The compaction process in a fully saturated material is intrinsically unstable and chemical compaction bands develop under stress. For large compaction values the regions between compacting layers fail in extension and generate open fractures which drain adjacent fluids with dissolved mineral species and hence develop into veins. If the alteration process is episodic then crack seal microstructures develop.

8.7. A synthesis.

Chemical reactions are of course a fundamental aspect of mineralised hydrothermal systems. However there is an important difference between the chemical evolution of open flow hydrothermal systems and closed metamorphic systems. Closed systems evolve to equilibrium whereas open systems are held far from equilibrium by the flow of nutrients, heat and momentum. The kinetics of closed metamorphic systems can be described at a macroscopic level by the rate constants of the individual reactions that occur in the system. However, since the rates of chemical reactions also depend on the rates at which mass and energy are added to the reaction site, the kinetics of open flow systems can only be described at the macroscopic level by also considering the rates at which chemical species, heat and momentum are added and removed from the system. Such an observation also applies to closed systems at the microscopic level but such processes are usually neglected by metamorphic petrologists.

In any system where multiple processes or chemical reactions occur, there is competition between the supply and consumption of mass and energy and the rates of growth and dissolution of mineral phases. The situation commonly arises where the rate of a particular process outstrips the supply of mass and/or energy. At that stage the particular process stops and resumes when the supply of relevant material or energy builds up again. Thus episodic (oscillatory, aperiodic or chaotic) processes are the norm in open flow systems; chaotic behaviour emerges if more than two processes compete for supply or consumption of mass or energy.

Hydrothermal systems are characterised by an early pervasive alteration of pre-existing mineral assemblages where the introduction of fluids such as CO_2 and H_2O react to produce carbonates (calcite, ankerite and siderite) and hydrous silicates (sericite, chlorite). Such reactions (together with those that produce oxides such as haematite) are strongly exothermic so that once the reaction system is nucleated the alteration process is self-sustaining or even self-enhancing governed solely by the rates at which fluids are added to the system or heat is removed from the system. These reaction rates are extremely sensitive to fluctuations in the rates of fluid and heat supply/removal. The spatio-temporal behaviour of such systems is intrinsically chaotic.

In principle the evolution of large exothermic systems such as large alteration systems corresponds to thermal runaway but the rise in temperature is capped by the initiation of endothermic processes corresponding to complete or partial dehydration and decarbonation of alteration phases generated earlier in the alteration history or the deposition of sulphides and metals such as gold. Thus pyrophyllite or K-feldspar overprints kaolinite, K-feldspar overprints annite or siderite overprints calcite. Again, these reactions are intrinsically chaotic both spatially and temporally.

In addition to the strong influence of the rates of heat and mass supply on the chemical behaviour of a hydrothermal system, the nonlinear nature of the exothermic chemical reactions leads to large fluctuations in temperature; again these fluctuations can be chaotic both spatially and temporally. Such episodic thermal behaviour leads to episodic fluctuations in fluid pressure; the effect is strongest at small spatial scales and in low permeability rocks. In undrained conditions the coefficient of thermal pressurisation is in the range 0.01 to 1 MPa/^{o}C so the effect is large.

Three types of feedback between mechanical behaviour and fluid pressure increases can be distinguished:

(i) For small increases in fluid pressure pre-existing veins can be opened with subsequent deposition of quartz or calcite during the relaxation phase of the temperature/pore fluid cycle. This leads to crack-seal microstructures.

(ii) For larger increases in fluid pressure such that the effective stress initiates fracture, brecciation occurs. Cementation again occurs during the relaxation phase of the temperature/fluid pressure cycle. This brecciation-cementation phase is overprinted as the episodic nature of the adjacent chemical reactions proceeds.

(iii) For large increases in fluid pressure such that the fluid pressure exceeds lithostatic complete fluidisation of the system occurs. Again this is episodic.

These mechanical processes, consisting mainly of rock breakage and sliding on fractures, are exothermic and lead to oscillatory (stick-slip) types of behaviour identical in principle to the episodic nature of chemical reactions. The heat produced by these mechanical processes is consumed in driving endothermic mineral reactions involving devolatilisation which in turn enhances the mechanical dissipation. The other fundamental endothermic processes that result from the chemo-mechanical coupling are the deposition of sulphides and gold.

The episodic evolution of fluid pore pressure and temperature in hydrothermal systems is the basis for gold deposition in vein systems. During the relaxation phase of each temperature/ore pressure cycle the solubility of gold decreases and situations may arise where boiling or phase separation occurs. These are the conditions for episodic deposition of gold and of quartz. In addition if pyrite or arseno-pyrite grows during the temperature increase phase of the cycle then the growth takes place in an environment where the solubility of gold in pore fluids is increasing. Gold is then incorporated into the growing pyrite thus leading to a refractory system. If however pyrite grows during the relaxation period the growth takes place in an environment where the gold solubility in pore fluid is decreasing leading to a non-refractory system.

Many alteration reactions involve volume loss or “chemical compaction”. Decarbonation of marbles has been estimated to produce up to 50% volume loss whereas the alteration reactions listed in Table 8.2 can potentially produce volume losses from the compacting band of up to 70%. The deformation of a fluid saturated system undergoing compaction is unstable and any perturbation in fluid pressure grows exponentially to form a spatial patterning of regions undergoing compaction and regions undergoing extensional strain. The extensional regions may be planar or more equant in shape. We propose that planar extensional regions in the compacting system become veins that open and close as the temperature/pore pressure oscillations occur. These oscillations are the origin of crack-seal microstructures and mark the deposition of gold in vein systems if the episodic system is associated with the devolatilisation of hydrous are carbonated assemblages previously formed in the low temperature phases of alteration. The result is a vein system embedded in the alteration system that underwent compaction.

In an open system even the simplest of mineral reactions is unstable if the growth of the product outstrips the supply of nutrients (or heat in the case of an endothermic reaction). For simple systems involving up to two processes (reaction plus supply of nutrients) the instabilities are expressed as periodic oscillations. If more than two processes operate (such as two exothermal reactions where competition for heat exists between two reactions) chaotic behaviour in both chemical concentrations and temperature/pore pressure is the response. We

have seen in Chapter 7 that chaotic systems produce responses that are multifractal in character. Hence we expect hydrothermal systems to be multifractal and the goal of any study of such systems is to decipher something of the origin and evolution of the system from the multifractal signature. We follow this line in detail in Chapters 9 and 10.

For the moment we speculate on the nature of the chaotic attractor that might be characteristic of hydrothermal systems. In Figure 8.12 (b, c, d) we show attractors produced by two simple exothermic reactions that are coupled solely through competition for the supply of heat. These attractors resemble what is known as a Rossler attractor and other reactions have been reported in the literature that produce this attractor. Some examples are shown in Figure 8.28. We propose that whilst the attractor trajectories remain more or less planar (as in Figures 8.28 a and b) the alteration/mineralisation signature gives relatively narrow multifractal singularity spectra. However once the attractor begins to expand into three dimensions (as in Figures 8.28 c and d) the signal becomes intermittent and the singularity spectrum widens. This latter behaviour is typical of gold distributions in large, high grade deposits whereas the former behaviour is typical of smaller low grade deposits. We expand on these concepts in Chapters 10 and 11. In Chapter 12 we discuss some attractors that result from a model of gold deposition resulting from episodic behaviour of coupled deformation – chemical reaction systems. Figure 8.29 is a suggestion of how the behaviour of such attractors is expressed in the distribution of alteration assemblages and gold distributions.

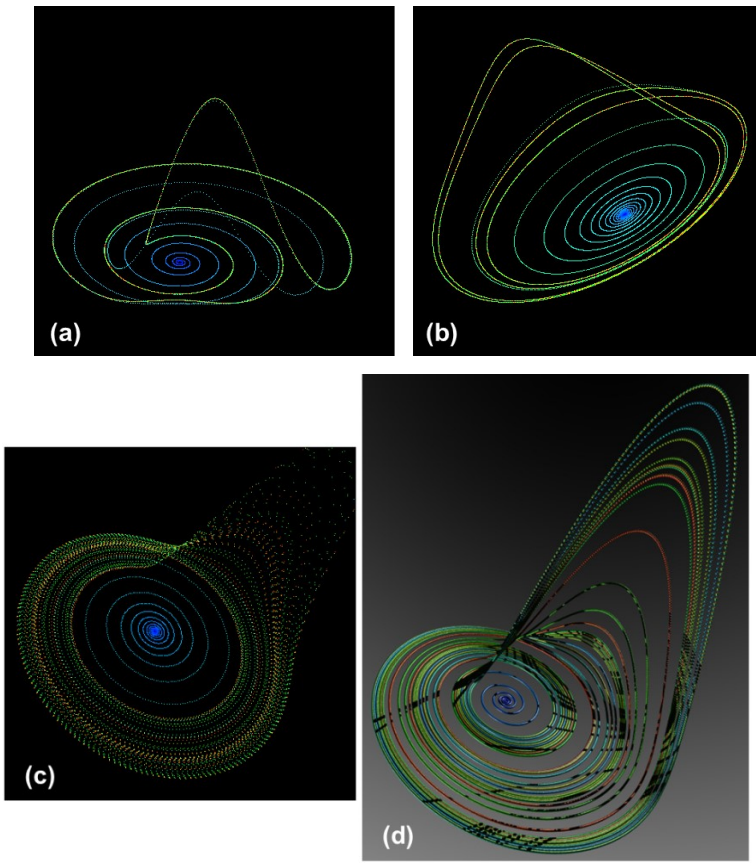

Figure 8.28. Images of the Rossler attractor (From Paul Bourke: http://paulbourke.net/fractals/rossler/). We propose that images (a) and (b) are representative of the behaviour of low grade gold deposits with no intermittency. Figures (c) and (d) are representative of large high grade gold deposits with well developed intermittency.

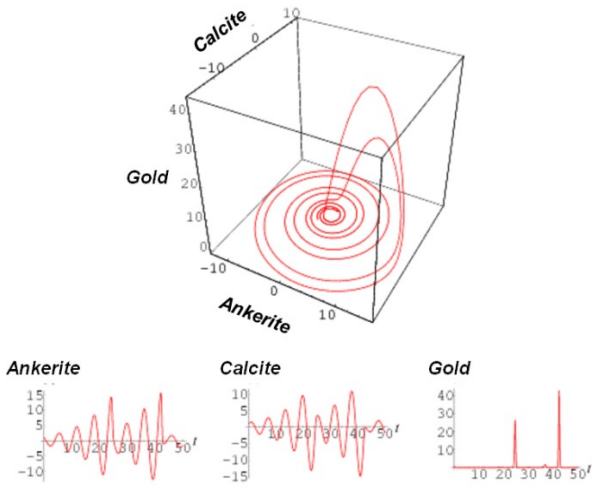

Figure 8.29. The geological manifestation of Figure 8.28. The Rossler attractor is a plot of (say) calcite, ankerite, and gold concentrations with time. The concentration evolution for these three minerals is shown below the attractor. The gold shows intermiitent behaviour, characteristic of large well endowered deposits. Calcite and ankerite oscillate but show no apparent relationship to gold even though in fact there is a strong genetic relationship. For less endowered gold deposits the attractor does not show these large excursions into gold concentration space and resembles more Figure 8.28 (a).

Recommended reading.